Arch. Mech., **53**, 4-5, pp. 385–420, Warszawa 2001

Transport phenomena in saturated porous media undergoing liquid-solid phase change

C. GEINDREAU and J.-L. AURIAULT

Laboratoire "Sols, Solides, Structures" (3S)
UJF, INPG, UMR CNRS 5521,
BP 53X 38041 Grenoble Cedex 09, France.

THE MACROSCOPIC MODELLING of transport phenomena occurring during the solidification process in porous media is revisited in this paper. The particular case of binary phase change in metallic alloys is considered. Continuum models for momentum, mass, heat and species transport in metallic saturated porous media undergoing liquid-solid phase change are derived from the description at the pore scale by using an upscaling technique. We use the method of multiple scale expansions which gives rigorously the macroscopic behaviour. Different macroscopic descriptions are derived in function of the orders of magnitude of dimensionless numbers that characterize the dominating phenomena and the physical properties of the constituents at the microscopic scale. Among the distinct homogenizable situations, the three richest cases are presented in this paper. The domains of validity of the micro-macrosegregation models, i.e lever-rule type models and Scheil type models, are shown by means of the order of magnitude of dimensionless numbers. The continuous passage between the different models is investigated.

Key words: porous media; heat transfer; mass transport; species transport; phase change; metallic materials, solidification, homogenisation.

Notations

$\mathbf{b}$	pore vector field
C_p^s, C_p^f	solid and fluid thermal capacities [J/(kg.K)]
D^s, D^f	solid and fluid diffusion coefficients [m^2/s]
D, K, M, Q, H, W	dimensionless numbers
$\mathbf{D}^*$	effective diffusion tensors [m^2/s]
$\mathbf{D}^{**}$	effective dispersion tensors [m^2/s]
f^s, f^f	solid and fluid volume fractions [dimensionless]
FT^s, FT^f	solid and fluid thermal Fourier numbers [dimensionless]
FS^s, FS^f	solid and fluid solutal Fourier numbers [dimensionless]
$k(T^*)$	equilibrium partition ratio [dimensionless]
$\mathbf{k}, \mathbf{K}$	microscopic and macroscopic permeability tensors [m^2]
l	characteristic microscopic length [m]
L^{fs}	latent heat of fusion [J/kg]

L	characteristic macroscopic length [m]
Le^s, Le^f	solid and fluid Lewis numbers [dimensionless]
$\mathbf{N}$	unit outward vector of Γ
p^f	fluid pressure [Pa]
PT^f	thermal Péclet number of the fluid phase [dimensionless]
PS^f	solutal Péclet number of the fluid phase [dimensionless]
Re	Reynolds number [dimensionless]
REV	Representative Elementary Volume
t	time [s]
T^s, T^f	solid and liquid temperatures [K]
$\mathbf{v}^s, \vec{v}^f$	solid and fluid velocities [m/s]
$\mathbf{w}$	liquid-solid interface velocity [m/s]
$\mathbf{X}$	physical space variable [m]
$\mathbf{x}$	macroscopic (or slow) space variable [dimensionless]
$\mathbf{y}$	microscopic (or fast) space variable [dimensionless]

Greek letters

β, φ, χ	pore vector fields
Γ	boundary between Ω^s and Ω^f
δ	unit tensor
λ^{eff}	effective thermal conductivity tensor [J/(m.K.s)]
ε	parameter of scale separation [dimensionless]
λ^s, λ^f	solid and fluid thermal conductivity [J/(m.K.s)]
μ^f	solid and fluid viscosity [Pa.s]
ρ^s, ρ^f	solid and fluid densities [kg/m^3]
ϕ, Φ	complex functions
ω^s, ω^f	fluid and solid mass fractions [dimensionless]
Ω	total volume of the periodic cell [m^3]
Ω^f, Ω^s	solid and fluid volumes of the periodic cell [m^3]
∇	gradient operator
$\nabla\cdot$	divergence operator

Subscripts

c	characteristic quantities related to the physical phenomenon
l	dimensionless number using l as reference length
x	macroscopic variable in use for derivation
y	microscopic variable in use for derivation

Superscripts

$*$	interfacial value (Γ)
s	value defined in Ω^s
f	value defined in Ω^f

1. Introduction

THE STUDY OF SOLID-LIQUID phase change in fluid-saturated porous media that involve coupled mass transport, heat transfer, fluid flow and species transport processes, spans a range of scientific and engineering domains, including metallurgy, material sciences and earth sciences. For example, such research is necessary to predict the formation of defects in mechanical components due to micro- or macrosegregation occurring during casting processes [9,26,25,15,20], or to describe the formation of the various igneous rocks in geological systems [14,7,13]. In nuclear engineering, it is also fundamental to describe correctly the solidification of a molten pool, namely the corium, that can be found in a nuclear vessel during a hypothetical accident [32].

The solidification of melts of many types of materials, as metals and igneous rocks, leads to the formation of a mushy zone [9] which separates the fully solidified and melted regions during solidification. The mushy zone is composed of solid dendrites and interdendritic liquid. In most solidification models, the mushy zone is viewed as a saturated porous medium undergoing liquid-solid phase change [20]. In order to simulate solidification processes, two different approaches have been adopted in the past: the multi-domain approach and the single-domain approach. In the multi-domain approach, the conservation equations for the solid phase and the fluid phase are solved separately with appropriate boundary conditions over the moving solid-liquid interface [28,29,23,31]. Due to the complex interfacial geometry that characterizes the solidification of multi-component systems, it is usually difficult to solve the problem without any questionable hypothesis. For these reasons, the single-domain approach is usually preferred. In this approach, the multi-component system is viewed as a continuum material described by a single set of conservation equations for the whole domain comprising the solid, the mush and the fluid domains. In the last two decades, several continuum transport models have been developed using the mixture theory [14,5,12,30,21] and the volume average method [4,10,22,19]. Most of them concern the binary phase change such as in metallic alloys and have been applied to simulate solidification processes such as casting or welding. It is well known that macroscopic description of the solidification process strongly depends on the physical properties of each phase and on the physical processes at the microscopic scale [20]. Hence, the macroscopic description can take different forms according to the intensity of the phenomena occurring at the microscopic scale. Although the mixture theory and the volume average approach allow to capture some microscopic information at the macroscopic scale, macroscopic prerequisites are sometimes required for deriving the different macroscopic description. Moreover, the domain of validity of the derived macroscopic models and homoge-

nisability conditions, i.e conditions under which an equivalent macroscopic description exists, are not expressly stated.

The macroscopic modelling of transport phenomena occurring during the solidification process in porous media is revisited in this paper by using the homogenisation method of multiple scale expansions [6,24,1]. The particular case of binary phase change in metallic alloys is considered. The upscaling technique we are using allows to derive the macroscopic behaviour from the description of the physical mechanisms at the microscopic scale without any prerequisite of the form of the macroscopic equations. The basic assumption of the method is the existence of a Representative Elementary Volume (REV) of the medium, which is large enough to be a representative of the heterogeneity scale and small in comparison with the macroscopic volume. We also assume the medium to be periodic. In a periodic medium, the periodic cell represents the REV. Let l be the characteristic length of the REV and L be the characteristic macroscopic dimension. The key parameter of the upscaling method is the small parameter

$$\varepsilon = \frac{l}{L} \ll 1. \tag{1.1}$$

ε is the parameter of scale separation. The separation of scales must also be verified regarding the phenomenon. Under these conditions, the corresponding macroscopic descriptions are intrinsic to the geometry of the medium and the phenomenon. They are also independent of the macroscopic boundary conditions. In this study, we follow the approach suggested in [1].It enables to obtain the macroscopic laws, their domain of validity and also the effective parameters. Homogenisability conditions are also expressly stated. The methodology is based on the definition and estimation of dimensionless numbers that characterize the dominating phenomena and the physical properties of the constituents at the microscopic scale. The domain of validity of the derived macroscopic description is given by means of orders of magnitude of the local dimensionless numbers.

The existence of a REV plus a scale separation are the necessary conditions for the existence of an equivalent macroscopic description. Although the dendritic skeleton is nonuniform and anisotropic in the the mushy zone [20], we will admit these two conditions to be fulfilled. If they are not verified, there is no possible equivalent macroscopic description.

The physics at the microscopic scale of a binary-alloy solidification system is presented in Sec. 2. Section 3 is devoted to the estimations of the dimensionless numbers arising from the description at the microscopic scale with respect to the scale ratio ε. The homogenisation technique of multiple scale expansions for periodic structures is then applied in Sec. 4 to derive the macroscopic coupled equations of momentum, mass, heat and species transports. Among the different homogenisable situations, the three most fruitful cases are presented. The con-

tinuous passage between the different macroscopic models is investigated in the conclusion.

2. Description at the microscopic scale

The homogenisation method for periodic structures is applied to the solidification of a binary alloy A-B. Although the dendritic skeleton is nonuniform and anisotropic [20], the mushy zone (Fig. 1) is considered to be a periodic porous medium with a space period Ω.

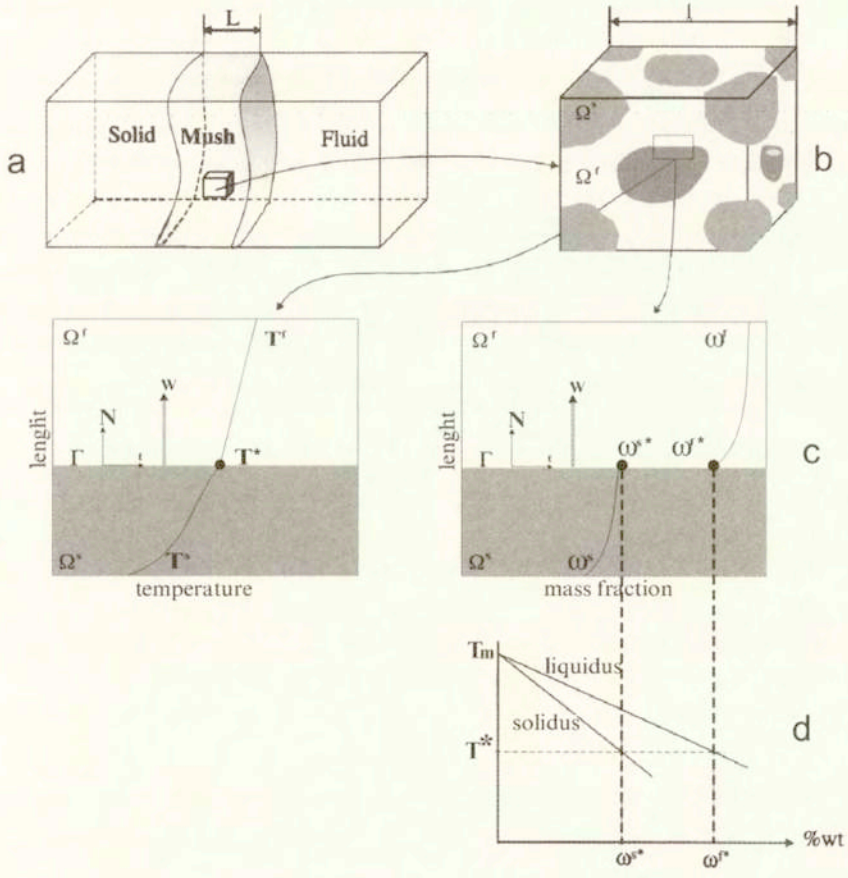

FIG. 1. (**a**) Macroscopic mushy zone with a large number of Representative Elementary Volumes or periodic cell. (**b**) Representative Elementary Volume or periodic cell Ω. (**c**) Schematic representation of the different boundary conditions on Γ. (**d**) Equilibrium phase diagram of a binary system.

This assumption is actually not a restriction [1,16]. The characteristic length of the period l is of about the same order of magnitude as the dimension of the pores or dendritic particles, while the scale L reveals the dimension of the mushy zone. Under typical solidification conditions in a metallic alloy system, a characteristic value of l is $l \approx 10^{-4}$m while $L \approx 10^{-1}$m, therefore $\varepsilon \approx 10^{-3}$. In the analysis to follow, this value for the separation of scales is adopted. Ω^s and Ω^f are the domains occupied by the solid phase (^{s}) and the fluid phase (^{f}), respectively. Each phase is assumed to be connected. The common boundary between solid and fluid is denoted Γ. At the microscopic scale, i.e at the REV scale, the medium is assumed to be composed of a fluid and of a rigid solid with phase change through which heat and species are diffused and are convected. The physical phenomena are governed by the following equations.

Momentum balance: At the microscopic scale, the solid skeleton is incompressible and usually follows a non-linear viscous law such as the Odqvist law. It has been shown that the motion of the solid network can play a key role in the fluid segregation, depending on the contrast of the mechanical properties of the solid and the fluid phases [11]. For the sake of simplicity, we assume in this study that the solid network is rigid ($\mathbf{v}^s = 0$). The fluid is considered to be an incompressible Newtonian fluid of viscosity μ^f. In the pores, the steady state fluid flow is governed by the usual Stokes equation,

$$\mu^f \triangle \mathbf{v}^f - \nabla p^f - \rho^f (\mathbf{v}^f \cdot \nabla)\mathbf{v}^f = 0. \tag{2.1}$$

$\mathbf{v}^f$ is the fluid velocity, p^f is the fluid pressure and ρ^f is the density of the fluid. In practice, μ^f and ρ^f depend on the temperature and the mass fraction of the different species (A-B). In this study, they are assumed to be constant.

Mass balance: The density of the solid phase, ρ^s ($\rho^s > \rho^f$), is also supposed to be constant. The incompressibility of the fluid is given by

$$\nabla \cdot \mathbf{v}^f = 0. \tag{2.2}$$

Energy balance: The heat transfer is governed by conduction in the solid phase whereas it is governed by conduction and convection in the fluid phase,

$$\rho^s C_p^s \frac{\partial T^s}{\partial t} - \nabla \cdot (\lambda^s \nabla T^s) = 0, \tag{2.3}$$

$$\rho^f C_p^f \frac{\partial T^f}{\partial t} + \rho^f C_p^f \vec{v}^f \cdot \nabla T^f - \nabla \cdot (\lambda^f \nabla T^f) = 0. \tag{2.4}$$

T^s and T^f are the temperature of the solid phase and the fluid phase, respectively. C_p^α and λ^α are the thermal capacity and the thermal conductivity of the

phase α ($\alpha = s, f$). In the following, C_p^α and λ^α are supposed to be independent of the temperature and of the mass fractions of the different species (A-B).

Species balance: Species transport is governed by diffusion in the solid phase and by diffusion and convection in the fluid phase,

$$\rho^s \frac{\partial \omega^s}{\partial t} - \nabla \cdot (\rho^s D^s \nabla \omega^s) = 0, \tag{2.5}$$

$$\rho^f \frac{\partial \omega^f}{\partial t} + \rho^f \mathbf{v}^f \cdot \nabla \omega^f - \nabla \cdot (\rho^f D^f \nabla \omega^f) = 0. \tag{2.6}$$

ω^α and D^α are the mass fraction and the diffusion coefficient of a given species (A or B) in the phase α ($\alpha = s, f$).

Conditions on the solid-liquid interface Γ: The following interfacial conditions are illustrated in Fig. 1.

- *Continuity of tangential velocities:*

$$\mathbf{v}^f \cdot \mathbf{t} = 0, \tag{2.7}$$

$\mathbf{t}$ is the unit tangential vector of Γ.

- *Continuity of mass fluxes:*

$$\rho^f (\mathbf{v}^f - \mathbf{w}) \cdot \mathbf{N} = -\rho^s \mathbf{w} \cdot \mathbf{N}, \tag{2.8}$$

where $\mathbf{N}$ is a unit outward vector of Γ and $\mathbf{w}$ is the velocity of the interface.

- *Continuity of temperatures:*

$$T^s = T^f = T^*. \tag{2.9}$$

A state of thermodynamic equilibrium is assumed. T^* is the equilibrium temperature on the interface.

- *Continuity of heat fluxes:*

$$\left(\lambda^s \nabla T^s - \lambda^f \nabla T^f\right) \cdot \mathbf{N} = L^{fs} \rho^s \mathbf{w} \cdot \mathbf{N}, \tag{2.10}$$

L^{fs} is the latent heat of fusion.

- *Continuity of species fluxes:*

$$\left(\rho^s D^s \nabla \omega^s - \rho^f D^f \nabla \omega^f\right) \cdot \mathbf{N} = (\rho^f \omega^{f*} - \rho^s \omega^{s*}) \mathbf{w} \cdot \mathbf{N}. \tag{2.11}$$

Under the assumption of thermodynamic equilibrium, the fluid mass fraction ω^{f*} and the solid mass fraction ω^{s*} on the interface Γ are related through the equilibrium phase diagram,

$$\omega^{s*} = k(T^*) \omega^{f*}, \tag{2.12}$$

where $k(T^*)$ is the equilibrium partition ratio. In this study, a linearised phase diagram is supposed, thus $k(T^*) = k$.

At the microscopic scale, the coupling between mass, heat and species transports is ensured by equations (2.8), (2.10)-(2.11) and the equilibrium phase diagram (2.12).

3. Homogenisation process

3.1. Normalisation

An important step of the homogenisation process is the normalisation of all equations. The above microscopic description (2.1)-(2.12) introduces fourteen dimensionless numbers that will measure the relative influence of the phenomena under consideration. From Eq. (2.1), we can define the Reynolds number Re and the dimensionless number Q^f,

$$Re = \frac{|\rho^f(\mathbf{v}^f \cdot \nabla)\mathbf{v}^f|}{|\mu^f \triangle \mathbf{v}^f|}, \qquad Q^f = \frac{|\nabla p^f|}{|\mu^f \triangle \mathbf{v}^f|}.$$

Eqs. (2.3)-(2.4) introduce two thermal Fourier numbers FT^s and FT^f, and the thermal Péclet number of the fluid phase PT^f,

$$FT^s = \frac{|\nabla \cdot (\lambda^s \nabla T^s)|}{\left|\rho^s C_p^s \dfrac{\partial T^s}{\partial t}\right|}, \quad FT^f = \frac{|\nabla \cdot (\lambda^f \nabla T^f)|}{\left|\rho^f C_p^f \dfrac{\partial T^f}{\partial t}\right|}, \quad PT^f = \frac{|\rho^f C_p^f \mathbf{v}^f \cdot \nabla T^f|}{|\nabla \cdot (\lambda^f \nabla T^f)|}.$$

Similarly, Eqs.(2.5)-(2.6) introduce two solutal Fourier numbers FS^s and FS^f, and the solutal Péclet number of the fluid phase PS^f,

$$FS^s = \frac{|\nabla \cdot (\rho^s D^s \nabla \omega^s)|}{\left|\rho^s \dfrac{\partial \omega^s}{\partial t}\right|}, \; FS^f = \frac{|\nabla \cdot (\rho^f D^f \nabla \omega^f)|}{\left|\rho^f \dfrac{\partial \omega^f}{\partial t}\right|}, \; PS^f = \frac{|\rho^f \mathbf{v}^f \cdot \nabla \omega^f|}{|\nabla \cdot (\rho^f D^f \nabla \omega^f)|}.$$

Now, from the continuity equation of mass fluxes (2.8) we obtain

$$M = \frac{|\mathbf{v}^f \cdot \mathbf{N}|}{|\mathbf{w} \cdot \mathbf{N}|}, \qquad R = \frac{\rho^s}{\rho^f}.$$

From the continuity equation of heat fluxes (2.10), we get the following two dimensionless numbers

$$K = \frac{\lambda^s}{\lambda^f}, \qquad H = \frac{|L^{fs}\rho^s \mathbf{w} \cdot \mathbf{N}|}{|\lambda^f \nabla T^f \cdot \mathbf{N}|}.$$

Finally, from the continuity equation of species fluxes (2.11), we have

$$D = \frac{D^s}{D^f}, \qquad W = \frac{|(\rho^f \omega^{f*} - \rho^s \omega^{s*})\mathbf{w} \cdot \mathbf{N}|}{|\rho^f D^f \nabla \omega^f \cdot \mathbf{N}|}.$$

Note that Re, Q^f, FT^s, FT^f, PT^f, FS^s, FS^f, PS^f are defined in the bulk of each phase whereas M, R, K, H, D and W are defined on the solid-liquid interface Γ.

3.2. Estimation of the dimensionless numbers

According the methodology presented in [1], the next important step of the homogenisation process consists in estimating these different dimensionless numbers arising from the description at the microscopic scale with respect to the key parameter ε of the process. In practice, ε is varying in time and in space because the mushy zone is expanding during the processes which changes l and L. Therefore estimation of dimensionless numbers may vary in time and space. Although we may consider several values of ε, we assume for simplicity in this study that $\varepsilon \approx 10^{-3}$, which corresponds to the situation of the greatest interest. Remark that macroscopic models already proposed are actually based on this typical value [20]. Let us consider l as the reference characteristic length. Thus, the microscopic point of view is adopted and the dimensionless numbers will be denoted by the subscript l. Notice that this choice does not affect the final result. Dimensionless numbers R_l, K_l, D_l can easily be estimated from the physical properties of the constituents. For example, from the material properties of a Pb-Sn alloy (Table 1), we have: $R_l = O(1)$, $K_l = O(1)$ and $D_l = O(\varepsilon)$. In the particular case of a Fe-C alloy (Table 1), R_l, K_l and D_l are $O(1)$. For the other dimensionless numbers, several orders of magnitude leading to several homogenisable situations may be considered. These numbers are expressed by means of characteristics quantities (denoted by the subscript c) that are related to the physical phenomenon (pressure drop, fluid velocity, solidification time ...).

The fluid flow and the mass balance depends on three dimensionless numbers,

$$Re = \frac{|\rho^f (\mathbf{v}^f \cdot \nabla)\mathbf{v}^f|}{|\mu^f \triangle \mathbf{v}^f|} \quad \Longrightarrow \quad Re_l = O\left(\frac{\rho_c^f v_c^f l}{\mu_c^f}\right),$$

$$Q^f = \frac{|\nabla p^f|}{|\mu^f \triangle \mathbf{v}^f|}. \quad \Longrightarrow \quad Q_l^f = O\left(\frac{p_c^f \; l}{\mu_c^f v_c^f}\right),$$

$$M = \frac{|\mathbf{v}^f \cdot \mathbf{N}|}{|\mathbf{w} \cdot \mathbf{N}|} \quad \Longrightarrow \quad M_l = O\left(\frac{v_c^f}{w_c}\right)_\Gamma.$$

Table 1. Physical properties of metallic alloys

Physical properties	Pb-Sn [15]	Fe-C [18]
ρ^s [kg/m^3]	10800	7300
ρ^f [kg/m^3]	10000	7300
μ^f [Pa.s]	10^{-3}	10^{-3}
C_p^f [J/(kg.K)]	177	800
C_p^s [J/(kg.K)]	154	800
D^s [m^2/s]	2.10^{-12}	10^{-10}
D^f [m^2/s]	10^{-9}	10^{-9}
λ^f [J/(m.K.s)]	22.9	30
λ^s [J/(m.K.s)]	39.7	30
^{fs} [J/kg]	30162	270000

Usually, the range of the fluid velocity in the mushy zone that is encountered in castings is between 10^{-7} m/s and 10^{-3} m/s. This corresponds to a variation of the Reynolds number from 0.001 to 1: $O(\varepsilon) \leq Re_l \leq O(1)$. For sufficiently low Reynolds numbers, $Re_l \approx O(\varepsilon)$, the steady state flow of an incompressible fluid through porous media is described by Darcy's law: the fluid velocity is linearly related to the gradient of the fluid pressure. As the Reynolds number increases, non-linearities appear and the drag law becomes nonlinear at the macroscopic scale [17, 27]. In this study, we will simply assume that Reynolds number is very small $Re_l \approx O(\varepsilon)$. On the other hand, it can be shown by a simple physical reasoning [1] that the problem is homogenisable if $Q_l^f = O(\varepsilon^{-1})$ and if the interfacial velocity is small or very small compared to the fluid velocity [3], i.e $M_l \geq O(\varepsilon^{-1})$.

Concerning the thermal problem, the microscopic description introduces four dimensionless numbers which can be estimated as follows

$$FT^s = \frac{|\nabla \cdot (\lambda^s \nabla T^s)|}{\left|\rho^s C_p^s \dfrac{\partial T^s}{\partial t}\right|} \quad \Longrightarrow \quad FT_l^s = O\left(\frac{\lambda_c^s \; t_c}{\rho_c^s \; C_{pc}^s \; l^2}\right),$$

$$FT^f = \frac{|\nabla \cdot (\lambda^f \nabla T^f)|}{\left|\rho^f C_p^f \dfrac{\partial T^f}{\partial t}\right|} \quad \Longrightarrow \quad FT_l^f = O\left(\frac{\lambda_c^f \; t_c}{\rho_c^f \; C_{pc}^f \; l^2}\right),$$

$$PT^f = \frac{|\rho^f C_p^f \, \mathbf{v}^f \cdot \nabla T^f|}{|\nabla \cdot (\lambda^f \nabla T^f)|} \quad \Longrightarrow \quad PT_l^f = O\left(\frac{\rho_c^f \; C_{pc}^f \; v_c^f \; l}{\lambda_c^f}\right),$$

$$H = \frac{|L^{fs} \rho^s \mathbf{w} \cdot \mathbf{N}|}{|\lambda^f \nabla T^f \cdot \mathbf{N}|} \quad \Longrightarrow \quad H_l = O\left(\frac{L_c^{fs} \; \rho_c^s \; w_c \; \delta_T^f}{\lambda_c^f \; \delta T^f}\right)_\Gamma .$$

t_c is the characteristic solidification time, δ_T^f is the fluid thermal diffusion layer thickness and $\delta T^f = |T^f - T^*|$ stands for the temperature increment in the boundary layer. Assuming that during castings, the range of the characteristic solidification time is typically between 10^2 s and 10^6 s, we have: $O(\varepsilon^{-2}) \leq FT_l^s \simeq FT_l^f \leq O(\varepsilon^{-3})$. The range of the fluid velocity implies that the thermal Péclet number of the fluid phase is small: $O(\varepsilon) \geq PT_l^f \geq O(\varepsilon^2)$. Consider now H_l. It has been shown [3] that the interface velocity must be small compared to the fluid velocity: $w_c \leq O(\varepsilon\, v_c^f)$. The fluid thermal-diffusion length δ_T is, in general, a complicated function of the microstructure, the solid volume fraction, interface velocities and curvatures, the time, melt flow conditions ... If we consider that $\delta_T^f \leq 10^{-5}$ m $\leq l$ and $\delta T^f \approx 10$ K, we get: $O(\varepsilon^3) \leq H_l \leq O(\varepsilon)$.

The microscopic dimensionless description of the species transport introduces four dimensionless numbers:

$$FS^s = \frac{|\nabla \cdot (\rho^s D^s \nabla \omega^s)|}{\left|\rho^s \dfrac{\partial \omega^s}{\partial t}\right|} \quad \Longrightarrow \quad FS_l^s = O\left(\frac{D_c^s\ t_c}{l^2}\right),$$

$$FS^f = \frac{|\nabla \cdot (\rho^f D^f \nabla \omega^f)|}{\left|\rho^f \dfrac{\partial \omega^f}{\partial t}\right|} \quad \Longrightarrow \quad FS_l^f = O\left(\frac{D_c^f\ t_c}{l^2}\right),$$

$$PT^f = \frac{|\rho^f \mathbf{v}^f \cdot \nabla \omega^f|}{|\nabla \cdot (\rho^f D^f \nabla \omega^f)|} \quad \Longrightarrow \quad PT_l^f = O\left(\frac{v_c^f\ l}{D_c^f}\right),$$

$$W = \frac{|(\rho^f \omega^{f*} - \rho^s \omega^{s*})\mathbf{w} \cdot \mathbf{N}|}{|\rho^f D^f \nabla \omega^f \cdot \mathbf{N}|} \quad \Longrightarrow \quad W_l = O\left(\frac{(\rho_c^f \omega_c^{f*} - \rho_c^s \omega_c^{s*})\ \delta_D^f\ w_c}{\rho_c^f\ D_c^f\ \delta\omega_c^f}\right)_\Gamma.$$

δ_D^f is the fluid-species diffusion length and $\delta\omega_c^f = |\omega^f - \omega^{f*}|$ stands for the fluid mass fraction increment in the boundary layer. Solutal dimensionless numbers can be related to thermal dimensionless numbers by introducing the fluid and the solid Lewis numbers defined as the ratio of the thermal diffusivity to the solutal diffusivity,

$$Le_l^f = O\left(\frac{\lambda_c^f}{\rho_c^f\ C_{pc}^f\ D_c^f}\right) = O(\varepsilon^{-1}),$$

$$Le_l^s = O\left(\frac{\lambda_c^s}{\rho_c^s\ C_{pc}^s\ D_c^s}\right) = O(Le_l^f\ D_l^{-1}).$$

Taking into account these results, we obtain: $O(\varepsilon^{-1}) \leq FS_l^f \simeq Le_l^{f-1}\ FT_l^f \leq O(\varepsilon^{-2})$, $FS_l^s \simeq D_l\ FS_l^f$ and $O(1) \geq PS_l^f \simeq Le_l^f\ PT_l^f \geq O(\varepsilon)$. It has been shown [2] that the problem is not homogenisable, i.e. an equivalent macroscopic

description does not exist, if $PS_l^f \geq O(\varepsilon^{-1})$. On the interface Γ, the fluid and solid mass fractions are related to the temperature through the equilibrium phase diagram. Thus, we get: $O(\varepsilon^2) \leq W_l \simeq Le_l^f \; H_l \leq O(1)$.

The above analysis shows that the dimensionless numbers arising from the description at the microscopic scale can take different orders of magnitude according to the physical properties of the constituents and to the characteristic quantities that are related to the physical phenomenon at the microscopic scale. Therefore, when applying the homogenisation process to the local description, it turns out that several macroscopic descriptions can be derived from the microscopic description according to the order of magnitude of these dimensionless numbers. Among the different homogenisable situations in which $PS_l^f < O(\varepsilon^{-1})$, $FS_l^f \geq O(\varepsilon^{-1})$ and $M_l \geq O(\varepsilon^{-1})$, only the three most fruitful cases (cases A, B and C) are presented in this paper. These three cases of interest (Fig. 2) correspond to different orders of dimensionless numbers, which are summarized in Table 2. Practical situations in which $PS_l^f \geq O(\varepsilon^{-1})$, $FS_l^f < O(\varepsilon^{-1})$ and $M_l < O(\varepsilon^{-1})$ can occur. However, in these cases an equivalent macroscopic description does not exist [1].

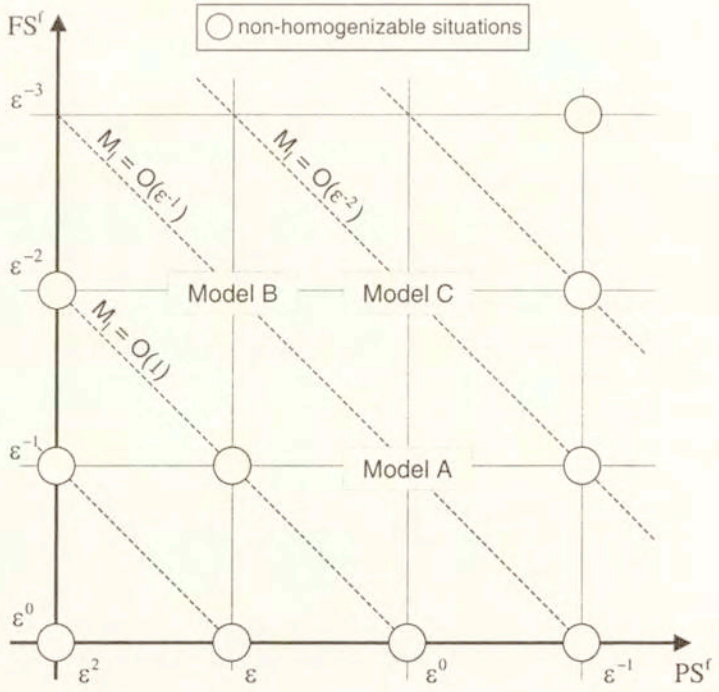

FIG. 2. Homogenizable and non-homogenizable situations with respect to the orders of magnitude of the three dimensionless numbers: M_l, FS_l^f and PS_l^f.

We are now able to write Eqs. (2.1)-(2.12) in the dimensionless form. For the sake of simplicity, we keep the same notations, but all quantities are now dimensionless quantities:

$$(3.1)\quad \mu^f \triangle \mathbf{v}^f - (Q^f)\,\nabla p^f - (Re)\,\rho^f(\mathbf{v}^f\cdot\nabla)\mathbf{v}^f = 0 \qquad \text{in } \Omega^f,$$

$$(3.2)\quad \nabla\cdot\mathbf{v}^f = 0 \qquad \text{in } \Omega^f,$$

$$(3.3)\quad (FT^s)^{-1}\,\rho^s C_p^s\frac{\partial T^s}{\partial t} - \nabla\cdot(\lambda^s\nabla T^s) = 0 \qquad \text{in } \Omega^s,$$

$$(3.4)\quad (FT^f)^{-1}\,\rho^f C_p^f\frac{\partial T^f}{\partial t} + (PT^f)\,\rho^f C_p^f\mathbf{v}^f\cdot\nabla T^f - \nabla\cdot(\lambda^f\nabla T^f) = 0 \qquad \text{in } \Omega^f,$$

$$(3.5)\quad (FS^s)^{-1}\,\rho^s\frac{\partial\omega^s}{\partial t} - \nabla\cdot(\rho^s D^s\nabla\omega^s) = 0 \qquad \text{in } \Omega^s,$$

$$(3.6)\quad (FS^f)^{-1}\,\rho^f\frac{\partial\omega^f}{\partial t} + (PS^f)\,\rho^f\mathbf{v}^f\cdot\nabla\omega^f - \nabla\cdot(\rho^f D^f\nabla\omega^f) = 0 \qquad \text{in } \Omega^f,$$

$$(3.7)\quad \mathbf{v}^f\cdot\mathbf{t} = 0 \qquad \text{on } \Gamma,$$

$$(3.8)\quad \rho^f((M)\,\mathbf{v}^f - \mathbf{w})\cdot\mathbf{N} = -(R)\,\rho^s\mathbf{w}\cdot\mathbf{N} \qquad \text{on } \Gamma,$$

$$(3.9)\quad T^s = T^f = T^* \qquad \text{on } \Gamma,$$

$$(3.10)\quad \Big((K)\,\lambda^s\nabla T^s - \lambda^f\nabla T^f\Big)\cdot\mathbf{N} = (H)\,L^{fs}\rho^s\mathbf{w}\cdot\mathbf{N} \qquad \text{on } \Gamma,$$

$$(3.11)\quad \Big((D)(R)\,\rho^s D^s\nabla\omega^s - \rho^f D^f\nabla\omega^f\Big)\cdot\mathbf{N} = (W)(\rho^f\omega^{f*} - \rho^s\omega^{s*})\mathbf{w}\cdot\mathbf{N} \qquad \text{on } \Gamma$$

$$(3.12)\quad \omega^{s*} = k\,\omega^{f*} \qquad \text{on } \Gamma$$

3.3. Homogenisation method of double scale expansions

The condition of separation of scales (1.1) enables us to use the homogenisation method of double scale expansions for periodic structures [6, 24, 1]. Both characteristic lengths L and l introduce two dimensionless space variables,

$$\mathbf{y} = \frac{\mathbf{X}}{l}, \qquad \mathbf{x} = \frac{\mathbf{X}}{L},$$

Table 2. Orders of magnitude of the dimensionless numbers corresponding to the three cases of interest: model A, B and C

	Model A	Model B	Model C
R_l	$O(1)$	$O(1)$	$O(1)$
K_l	$O(1)$	$O(1)$	$O(1)$
D_l	$O(1)$ or $O(\varepsilon)$	$O(1)$ or $O(\varepsilon)$	$O(1)$ or $O(\varepsilon)$
Re_l	$O(\varepsilon)$	$O(\varepsilon)$	$O(\varepsilon)$
Q_l^f	$O(\varepsilon^{-1})$	$O(\varepsilon^{-1})$	$O(\varepsilon^{-1})$
M_l	$O(\varepsilon^{-1})$	$O(\varepsilon^{-1})$	$O(\varepsilon^{-2})$
$FT_l^s \simeq FT_l^f$	$O(\varepsilon^{-2})$	$O(\varepsilon^{-3})$	$O(\varepsilon^{-3})$
PT_l^f	$O(\varepsilon)$	$O(\varepsilon^2)$	$O(\varepsilon)$
H_l	$O(\varepsilon^2)$	$O(\varepsilon^3)$	$O(\varepsilon^3)$
FS_l^f	$O(\varepsilon^{-1})$	$O(\varepsilon^{-2})$	$O(\varepsilon^{-2})$
$FS_l^s \simeq D_l FS_l^f$	$O(\varepsilon^{-1})$ or $O(1)$	$O(\varepsilon^{-2})$ or $O(\varepsilon^{-1})$	$O(\varepsilon^{-2})$ or $O(\varepsilon^{-1})$
PS_l^f	$O(1)$	$O(\varepsilon)$	$O(1)$
W_l	$O(\varepsilon)$	$O(\varepsilon^2)$	$O(\varepsilon^2)$

where $\mathbf{X}$ is the physical space variable. The variable $\mathbf{x}$ is the macroscopic (or slow) space variable and $\mathbf{y}$ is the microscopic (or fast) space variable. The unknown fields at the microscopic scale of a given boundary value problem appear as functions of these two dimensionless space variables and are looked for in the following forms,

$$\phi(\mathbf{x},\mathbf{y},t = \phi^{(0)}(\mathbf{x},\mathbf{y},t) + \varepsilon\phi^{(1)}(\mathbf{x},\mathbf{y},t) + \varepsilon^2\phi^{(2)}(\mathbf{x},\mathbf{y},t) + \cdots, \tag{3.13}$$

where $\phi(\mathbf{x},\mathbf{y},t) = p^f, \mathbf{v}^f, \mathbf{w}, T^f, T^s, \omega^f, \omega^s$ and the $\phi^{(i)}$ are periodic functions or vectors of period Ω with respect to space variable $\mathbf{y}$. Since l is the reference characteristic length, the corresponding dimensionless space variable is $\mathbf{y}$ and $\mathbf{x} = \varepsilon\mathbf{y}$. Thus, the gradient operator ∇ is now written $(\nabla_y + \varepsilon\nabla_x)$ where subscripts x and y denote the variable for the derivative. The methodology of the homogenisation consists in introducing the asymptotic expansions (3.13) in the dimensionless local description (3.1)-(3.12). Solving the boundary-value problems arising at the successive orders of ε leads to the macroscopic description.

4. Description at the macroscopic scale

4.1. Model A

We consider here the orders of magnitude of dimensionless numbers given in Table 2 for model A. The first order macroscopic description derived from the

microscopic equations is presented below. The detailed calculus is itemized in Appendix A.

Fluid flow and mass balance: At the first order of approximation, the fluid pressure (A.14) is constant over the periodic cell and the macroscopic fluid pressure gradient $\nabla_x p^{f(0)}$ is acting as a driving force for the local flow (A.19):

$$p^{f(0)} = p^{f(0)}(\mathbf{x}, t), \qquad \mathbf{v}^{f(0)} = -\mathbf{k}(\mathbf{y}, t)\nabla_x p^{f(0)}.$$

$\mathbf{k}(\mathbf{y}, t)$ is the microscopic permeability tensor solution of the boundary value problem (A.21)-(A.23). The macroscopic fluid velocity which is obtained by volume averaging follows the Darcy's law,

$$\langle \mathbf{v}^{f(0)} \rangle = -\mathbf{K}\nabla_x p^{f(0)}, \quad K_{ij} = \frac{1}{\Omega}\int_{\Omega^f} k_{ij}(\mathbf{y}, t)\, d\Omega, \tag{4.1}$$

where $\mathbf{K}$ is the macroscopic permeability tensor of the porous medium. The first order macroscopic volume balance takes the classical form (A.30),

$$\nabla_x \cdot \langle \mathbf{v}^{f(0)} \rangle + \left(\frac{\rho^s}{\rho^f} - 1\right)\frac{df^s}{dt} = 0, \tag{4.2}$$

where f^s is the solid volume fraction. The first term and the second term of this equation are equal to the fluid flux and the shrinkage due to the solidification process, respectively (open system). Let us remark that the shrinkage due to the solidification process appears at the macroscopic scale although the metallic fluid is incompressible at the microscopic scale (2.2).

Heat transfer: At the first order of approximation, we have only one temperature field which is constant over the periodic cell: $T^{s(0)} = T^{f(0)} = T^{*(0)} = T^{(0)}(\mathbf{x}, t)$. The macroscopic heat transfer is governed by Eq.(A.48),

$$(\rho C_p)^{\text{eff}}\,\frac{\partial T^{(0)}}{\partial t} + \rho^f C_p^f \mathbf{V}_T^{\text{eff}} \cdot \nabla_x T^{(0)} - \nabla_x \cdot \left(\boldsymbol{\lambda}^{\text{eff}} \nabla_x T^{(0)}\right) - L^{fs}\rho^s \frac{df^s}{dt} = 0. \tag{4.3}$$

$(\rho C_p)^{\text{eff}}$ and $\boldsymbol{\lambda}^{\text{eff}}$ are the effective thermal capacity and the effective thermal conductivity tensor of the mixture, respectively. $\mathbf{V}_T^{\text{eff}}$ is an effective fluid velocity which is different from the Darcy velocity (4.2) and which accounts for heat effects. Such velocity was already introduced in previous works [8]. These effective

parameters characterize the average properties of the medium at the macroscopic scale. They are defined as follows:

$$(\rho C_p)^{\text{eff}} = f^s \rho^s C_p^s + f^f \rho^f C_p^f, \tag{4.4}$$

$$\boldsymbol{\lambda}^{\text{eff}} = \frac{1}{\Omega} \int_{\Omega^f} \lambda^f \left(\nabla_y \boldsymbol{\chi} + \boldsymbol{\delta}\right) d\Omega + \frac{1}{\Omega} \int_{\Omega^s} \lambda^s \left(\nabla_y \boldsymbol{\chi} + \boldsymbol{\delta}\right) d\Omega, \tag{4.5}$$

$$\mathbf{V}_T^{\text{eff}} = \frac{1}{\Omega} \int_{\Omega^f} \mathbf{v}^{f(0)} \left(\nabla_y \boldsymbol{\chi} + \boldsymbol{\delta}\right) d\Omega. \tag{4.6}$$

where $\boldsymbol{\chi}(\mathbf{y}, t)$ is the solution to the boundary value problem (A.41)-(A.43). The macroscopic heat transfer is governed by conduction and convection incorporating a heat flux due the solidification process over the solid-liquid interface. The above macroscopic description corresponds to the most general regime and reveals a coupling between heat and mass transfer. The structure of the macroscopic model is similar to the structure of the macroscopic heat transfer model already derived by NI and BECKERMANN [19] using the volume average method.

Species transport:

CASE. $D_l = O(1)$ and $FS_l^s = O(\varepsilon^{-1})$: In this case (Fe-C alloy), the solute is completely mixed in the fluid and the solid phases, i.e. we recover a lever-rule type model. The macroscopic species transport (A.63) is governed by convection and also contains a species flux due to the solidification process over the solid-liquid interface,

$$\rho^s \frac{\partial (f^s k\, \omega^{f(0)})}{\partial t} + \rho^f \frac{\partial ((1 - f^s)\omega^{f(0)})}{\partial t} + \rho^f \langle \mathbf{v}^{f(0)} \rangle \cdot \nabla_x \omega^{f(0)} = 0, \tag{4.7}$$

$\omega^{s(0)}$ and $\omega^{f(0)}$ which are completely mixed in the fluid and the solid phases respectively, are related to the temperature $T^{(0)}$ through the equilibrium phase diagram and satisfy $\omega^{s(0)}(\mathbf{x}, t) = k\, \omega^{f(0)}(\mathbf{x}, t)$. Thus the system (4.1), (4.2), (4.3) and (4.7) is closed.

CASE. $D_l = O(\varepsilon)$ and $FS_l^s = O(1)$: In this case (Sn-Pb alloy), the solute is completely mixed in the fluid phase only, i.e. we recover a Scheil-type behaviour: $\omega^{f(0)} = \omega^{f(0)}(\mathbf{x}, t)$ and $\omega^{s(0)} = \omega^{s(0)}(\mathbf{x}, \mathbf{y}, t)$. The macroscopic species transport is now given by equation (A.73),

$$\rho^s \left(\left\langle \frac{\partial \omega^{s(0)}}{\partial t} \right\rangle + \frac{\mathrm{d} f^s}{\mathrm{d} t} \omega^{s*(0)} \right) + \rho^f \frac{\partial \left((1 - f^s)\omega^{f(0)} \right)}{\partial t} + \rho^f \langle \mathbf{v}^{f(0)} \rangle \cdot \nabla_x \omega^{f(0)} = 0, \tag{4.8}$$

where

$$(4.9)\quad \left\langle \frac{\partial \omega^{s(0)}}{\partial t} \right\rangle = \frac{1}{\Omega} \int_{\Omega^s} \frac{\partial \omega^{s(0)}(\mathbf{x}, \mathbf{y}, t)}{\partial t}\, d\Omega = \frac{1}{\Omega} \int_{\Omega^s} \nabla_y \cdot \left(D^s \nabla_y \omega^{s(0)} \right) d\Omega.$$

$\omega^{s*(0)}$ and $\omega^{f(0)}$ are also related to the temperature $T^{(0)}$ through the equilibrium phase diagram and satisfy $\omega^{s*(0)}(\mathbf{x}, t) = k\ \omega^{f(0)}(\mathbf{x}, t)$. Thus the system (4.1), (4.2), (4.3) and (4.8) is closed. The macroscopic species transport is governed by convection and solute "back diffusion" within the solid phase (4.9) which, in contrast with what is usually assumed, is not negligible. The macroscopic description also contains a species flux due to the solidification process over the solid-liquid interface. The solute "back diffusion" within the solid phase (4.9), i.e. the memory effects, can be expressed as follows

$$(4.10)\quad \left\langle \frac{\partial \omega^{s(0)}}{\partial t} \right\rangle = F^{-1}(\Phi(\omega)) * \omega^{f(0)}$$

where $F^{-1}(\Phi(\omega))$ in the inverse Fourier transform of $\Phi(\omega)$ and $*$ is the convolution product. $\Phi(\omega)$ is a complex effective coefficient given by Eq.(A.74),

$$(4.11)\quad \Phi(\omega) = \frac{1}{\Omega} \int_{\Omega^s} i\ \omega\ \phi(\omega, \mathbf{y})\ d\Omega$$

where $\phi(\omega, \mathbf{y})$ is the $\mathbf{y}$-periodic solution of the boundary value problem (A.69)-(A.70)

The above analysis shows that the macroscopic species transport equation takes two different forms according to the order of magnitude of the solutal Fourier number of the solid phase FS_l^s. This solutal Fourier number is estimated with respect to the parameter of scale separation, ε. The macroscopic description is given by a Scheil type model (4.8) and by a lever-rule type model (4.7) for small and large solutal Fourier number of the solid phase, respectively. In contrast with the macroscopic descriptions already proposed [9,5,22,19], the derived first order macroscopic models (4.7) and (4.8) do not contain the term $\rho^f \omega^{f(0)} \nabla_x \cdot \langle \mathbf{v}^{f(0)} \rangle$, although the shrinkage due to the solidification process appears at the macroscopic scale (4.2). This term characterizes the second order effects ($O(\varepsilon^2)$) in Eqs.(4.7) and (4.8). This result is due to the homogenisability condition: $M_l \geq O(\varepsilon^{-1})$. Practical situations in which $M_l < O(\varepsilon^{-1})$ can occur. However, in these cases an equivalent macroscopic description does not exist [3].

4.2. Model B

We now assume that the fluid velocity and the solidification process are very slow. Under such conditions, the three dimensionless numbers, Re_l, Q_l^f

and M_l are unchanged. Fourier numbers (FT_l^s, FT_l^f, FS_l^s, FS_l^f) are increased by an order of magnitude whereas Péclet numbers (PT_l^f, PS_l^f) and interfacial dimensionless numbers (H_l, W_l) are decreased by an order of magnitude (see Table 2 and Fig. 2). The derived macroscopic description is presented below.

Fluid flow and mass balance: The problem concerning the fluid flow and the mass balance is the same as in Model A. Once again, the fluid flow follows Darcy's law (4.1) and the macroscopic volume balance is given by Eq. (4.2).

Heat transfer: By following the same route as in Appendix A, it can be shown that the first-order macroscopic heat transfer is now governed by conduction only,

$$\nabla_x \cdot \left(\boldsymbol{\lambda}^{\text{eff}} \nabla_x T^{(0)}\right) = 0, \tag{4.12}$$

where $\boldsymbol{\lambda}^{\text{eff}}$ is the effective thermal conductivity tensor of the mixture already defined by Eq.(4.5)

Species transport:

CASE. $D_l = O(1)$ and $FS_l^s = O(\varepsilon^{-2})$ (Fe-C alloy): Under such conditions, the first order macroscopic description (Appendix B) is given by a lever-type model. The macroscopic species transport is now governed by diffusion and convection incorporating a species flux due to the solidification process over the solid-liquid interface,

$$\rho^s \frac{\partial(f^s k\, \omega^{f(0)})}{\partial t} + \rho^f \frac{\partial((1-f^s)\omega^{f(0)})}{\partial t} + \rho^f \mathbf{V}_S^{\text{eff}} \cdot \nabla_x \omega^{f(0)} - \nabla_x \cdot \left((\rho \mathbf{D}^\star) \nabla_x \omega^{f(0)}\right) = 0, \tag{4.13}$$

$\omega^{f(0)}$ and $\omega^{s(0)}$ are related to the temperature $T^{(0)}$ through the equilibrium phase diagram and satisfy $\omega^{s(0)}(\mathbf{x}, t) = k\ \omega^{f(0)}(\mathbf{x}, t)$. Thus the system (4.1), (4.2), (4.12) and (4.13) is closed. $\mathbf{V}_S^{\text{eff}}$ is an effective fluid velocity which is different from the Darcy velocity (4.1) and which accounts for solutal effects. The effective fluid velocity $\mathbf{V}_S^{\text{eff}}$ and the effective diffusion tensor $(\rho \mathbf{D}^\star)$ of the mixture are defined as follows:

$$\mathbf{V}_S^{\text{eff}} = \frac{1}{\Omega} \int_{\Omega^f} \mathbf{v}^{f(0)} \left(\nabla_y \boldsymbol{\beta}^f + \boldsymbol{\delta}\right) d\Omega,$$

$$(\rho \mathbf{D}^\star) = \frac{1}{\Omega} \int_{\Omega^f} \rho^f D^f \left(\nabla_y \boldsymbol{\beta}^f + \boldsymbol{\delta}\right) d\Omega \frac{1}{\Omega} \int_{\Omega^s} \rho^s D^s k\ \left(\nabla_y \boldsymbol{\beta}^s + \boldsymbol{\delta}\right) d\Omega.$$

$\boldsymbol{\beta}^s(\mathbf{y},t)$ and $\boldsymbol{\beta}^f(\mathbf{y},t)$ are the solutions to the boundary-value problem (B.16 - B.19). Once again, the homogenisability condition, $M_l \geq O(\varepsilon^{-1})$, implies that the term $\rho^f \omega^{f(0)} \nabla_x \cdot \mathbf{V}_S^{\text{eff}}$ does not appear in the first order derived macroscopic description (4.13).

CASE. $D_l = O(\varepsilon)$ and $FS_l^s = O(\varepsilon^{-1})$ (Sn-Pb alloy): It can be shown that macroscopic species transport is also given by Eq. (4.13). But now, the effective diffusion tensor is written,

$$(\rho \mathbf{D}^\star) = \frac{1}{\Omega} \int_{\Omega^f} \rho^f D^f \left(\nabla_y \boldsymbol{\beta}^f + \boldsymbol{\delta} \right) d\Omega.$$

4.3. Model C

In this last case, the solidification process is assumed to be very slow whereas the fluid velocity is increased by an order of magnitude. Consequently, the interfacial dimensionless number M_l and Péclet numbers (PT_l^f, PS_l^f) are increased by one order of magnitude whereas other dimensionless numbers remain unchanged (see Table 2 and Fig. 2 : model C). Under such conditions, the first-order macroscopic description is written as follows.

Fluid flow and mass balance: At the macroscopic scale, the fluid flow is always described by the Darcy law (4.1). The interface velocity is now very small compared to the fluid velocity ($M_l = O(\varepsilon^{-2})$). Therefore, the macroscopic volume balance takes the form

$$\nabla_x \cdot \langle \mathbf{v}^{f(0)} \rangle = 0. \tag{4.14}$$

The shrinkage due the solidification process does not appear at the macroscopic scale at the first order of approximation (closed system).

Heat transfer: By following the same route as in Appendix A, we obtain the first-order macroscopic description. The macroscopic heat transfer is governed by both conduction and convection,

$$\rho^f C_p^f \mathbf{V}_T^{\text{eff}} \cdot \nabla_x T^{(0)} - \nabla_x \cdot \left(\boldsymbol{\lambda}^{\text{eff}} \nabla_x T^{(0)} \right) = 0. \tag{4.15}$$

$\boldsymbol{\lambda}^{\text{eff}}$ and $\mathbf{V}_T^{\text{eff}}$ are the effective conductivity tensor of the mixture (4.5) and the effective fluid velocity (4.6), respectively.

Species transport:

CASE. $D_l = O(1)$ and $FS_l^s = O(\varepsilon^{-2})$ (Fe-C alloy): The solidification process is very slow. Thus, at the first order of approximation, the solute is completely mixed in the fluid and in the solid phase, i.e. we obtain a lever-type behaviour

(see Appendix C). The macroscopic species transport is governed by convection only,

$$\rho^f \langle \mathbf{v}^{f(0)} \rangle \cdot \nabla_x \omega^{f(0)} = 0, \tag{4.16}$$

with $\omega^{s(0)}(\mathbf{x}, t) = k\ \omega^{f(0)}(\mathbf{x}, t)$. In contrast with models A and B, the evolution of the solid volume fraction during the solidification process can not be deduced from the above macroscopic description at the first order of approximation. The evolution of the solid fraction may be derived from the second order macroscopic equation (C.26) governing the average fluid mass fraction $\langle \omega^f \rangle$ which is given by

$$\varepsilon\ \rho^s \frac{\partial (f^s k\ \langle \omega^f \rangle)}{\partial t} + \varepsilon\ \rho^f \frac{\partial ((1 - f^s) \langle \omega^f \rangle)}{\partial t} + \rho^f \langle \mathbf{v}^f \rangle \cdot \nabla_x \langle \omega^f \rangle - \varepsilon\ \nabla_x \cdot \Big((\rho \mathbf{D}^{\star\star}) \nabla_x \langle \omega^f \rangle \Big) = 0. \tag{4.17}$$

$\langle \omega^s \rangle$ and $\langle \omega^f \rangle$ are related to the macroscopic temperature $T^{(0)}$ through the equilibrium phase diagram and satisfy $\langle \omega^s \rangle = k\ \langle \omega^f \rangle$. Thus the system (4.2), (4.15), (4.16) and (4.18) is closed. $(\rho \mathbf{D}^{\star\star})$ is the effective dispersion tensor of the mixture,

$$(\rho \mathbf{D}^{\star\star}) = \frac{1}{\Omega} \int_{\Omega^f} \rho^f D^f \Big(\nabla_y \boldsymbol{\varphi}^f + \delta \Big)\, d\Omega + \frac{1}{\Omega} \int_{\Omega^f} \rho^f \mathbf{k} \nabla_x p^{f(0)} \cdot \boldsymbol{\varphi}^f\ d\Omega + \frac{1}{\Omega} \int_{\Omega^s} \rho^s D^s k\ \ (\nabla_y \boldsymbol{\varphi}^s + \delta)\, d\Omega,$$

where $\boldsymbol{\varphi}^f(\mathbf{y}, \nabla_x p^{f(0)}, t)$ and $\boldsymbol{\varphi}^s(\mathbf{y}, \nabla_x p^{f(0)}, t)$ are the solutions to the bounda- ry-value problem (C.17)-(C.20). The dispersive character of $(\rho \mathbf{D}^{\star\star})$ appears through its dependence on the macroscopic gradient of fluid pressure $\nabla_x p^{f(0)}$, i.e. the fluid velocity. $(\rho \mathbf{D}^{\star\star})$ is, in general, positive definite but it is nonsymmetric [2].

CASE. $D_l = O(\varepsilon)$ and $FS_l^s = O(\varepsilon^{-1})$ (Sn-Pb alloy): The macroscopic species transport is also given by equation (4.17). But now, the effective dispersion tensor is written in the form:

$$(\rho \mathbf{D}^{\star\star}) = \frac{1}{\Omega} \int_{\Omega^f} \rho^f D^f \Big(\nabla_y \boldsymbol{\varphi}^f + \delta \Big)\, d\Omega + \frac{1}{\Omega} \int_{\Omega^f} \rho^f \mathbf{k} \nabla_x p^{f(0)} \cdot \boldsymbol{\varphi}^f\ d\Omega.$$

5. Conclusion

Continuum models for momentum, mass, heat and species transport in metallic saturated porous media undergoing liquid-solid phase change have been rigorously derived from the description at the pore scale by using an upscaling

technique, namely the method of multiple scale expansions. Among the several homogenisable situations, the three most fruitful cases are presented. Their domain of validity is given by means of orders of magnitude of the dimensionless numbers characterizing the dominating phenomena and the physical properties of the constituents at the microscopic scale (Fig.2). In practical situations, knowledge of the order of magnitude of these dimensionless numbers will clearly indicate which model should be chosen for describing the physical processes.

In model A, fluid flow obeys Darcy's law and shrinkage effects due to the solidification process appear at the macroscopic scale (open system). Heat transfer is governed by conduction and convection incorporating a heat flux due to the liquid-solid phase change. We have shown that the species transport equation may take two different forms with respect to the orders of magnitude of the ratio of the solid diffusivity to the fluid diffusivity (D_l), i.e the solutal Fourier number of the solid phase (FS^s). For small solutal Fourier number of the solid phase, the macroscopic description is given by a Scheil type model: the species transport is governed by convection and solute "back diffusion" within the solid phase. It also contains a species flux due to the solidification process over the solid-liquid interface. For large solutal Fourier number of the solid phase, the macroscopic species transport follows a lever-rule type model.

In contrast with model A, we assume in model B that the solidification process and the fluid velocity are very slow. Under such conditions, the fluid flow follows Darcy's law and shrinkage effects due to the solidification process are still present at the macroscopic scale. The macroscopic heat transfer is governed by conduction only. For small and large solutal Fourier number of the solid phase, the macroscopic species transport follows a lever-rule type model and is governed by convection and diffusion.

In model C, the solidification process is considered to be very slow whereas the fluid velocity is increased by one order of magnitude. At the first order of approximation, the fluid flow obeys Darcy's law whereas shrinkage effects due the solidification process do not appear at the macroscopic scale (closed system). The macroscopic heat transfer is governed by conduction and convection. For small and large solutal Fourier number of the solid phase, the first order macroscopic species transport is governed by convection only. The evolution of the solid mass fraction can be deduced from the macroscopic description at the second order of approximation. In this case, the macro-segregation equation that governs the average fluid mass fraction contains both convection and dispersion terms.

There is a possible continuous passage from the mass transport models A and B to model C by increasing M_l (Fig. 2). Similarly, it can be shown that there exist continuous passages from heat transfer model A to models C and B. Model A corresponds to the most general regime. Concerning species transport, the only possible continuous passage is from model B to model C by increasing

the solutal Péclet number of the fluid phase PS^f and the dimensionless number M_l simultaneously (Fig. 2).

It should be mentioned that it is relatively straightforward to extend the models proposed in this paper to other solid-liquid systems (igneous rocks) and to more than two phases. For example, it would be very interesting to take into account the presence of a gas phase to describe correctly the formation of hot tears.

Appendix A. Model A

Taking into account the order of magnitude of the dimensionless numbers (see Table 2), the dimensionless description at the microscopic scale given by Eqs.(3.7)-(3.18), takes the form:

$$\mu^f \triangle \mathbf{v}^f - \varepsilon^{-1} \nabla p^f - \varepsilon \rho^f (\mathbf{v}^f \cdot \nabla)\mathbf{v}^f = 0 \qquad \text{in } \Omega^f, \tag{A.1}$$

$$\nabla \cdot \mathbf{v}^f = 0 \qquad \text{in } \Omega^f, \tag{A.2}$$

$$\varepsilon^2 \rho^s C_p^s \frac{\partial T^s}{\partial t} - \nabla \cdot (\lambda^s \nabla T^s) = 0 \qquad \text{in } \Omega^s, \tag{A.3}$$

$$\varepsilon^2 \rho^f C_p^f \frac{\partial T^f}{\partial t} + \varepsilon \rho^f C_p^f \mathbf{v}^f \cdot \nabla T^f - \nabla \cdot (\lambda^f \nabla T^f) = 0 \qquad \text{in } \Omega^f, \tag{A.4}$$

$$(FS_l^s)^{-1} \rho^s \frac{\partial \omega^s}{\partial t} - \nabla \cdot (\rho^s D^s \nabla \omega^s) = 0 \qquad \text{in } \Omega^s, \tag{A.5}$$

$$\varepsilon \rho^f \frac{\partial \omega^f}{\partial t} + \rho^f \mathbf{v}^f \cdot \nabla \omega^f - \nabla \cdot (\rho^f D^f \nabla \omega^f) = 0 \qquad \text{in } \Omega^f, \tag{A.6}$$

$$\mathbf{v}^f \cdot \mathbf{t} = 0 \qquad \text{on } \Gamma, \tag{A.7}$$

$$\rho^f (\varepsilon^{-1} \mathbf{v}^f - \mathbf{w}) \cdot \mathbf{N} = -\rho^s \mathbf{w} \cdot \mathbf{N} \qquad \text{on } \Gamma, \tag{A.8}$$

$$T^s = T^f = T^* \qquad \text{on } \Gamma, \tag{A.9}$$

$$\left(\lambda^s \nabla T^s - \lambda^f \nabla T^f\right) \cdot \mathbf{N} = \varepsilon^2 L^{fs} \rho^s \mathbf{w} \cdot \mathbf{N} \qquad \text{on } \Gamma, \tag{A.10}$$

$$\left((D_l)\ \rho^s D^s \nabla \omega^s - \rho^f D^f \nabla \omega^f\right) \cdot \mathbf{N} = \varepsilon(\rho^f \omega^{f*} - \rho^s \omega^{s*}) \mathbf{w} \cdot \mathbf{N} \qquad \text{on } \Gamma, \tag{A.11}$$

$$\omega^{s*} = k\ \omega^{f*} \qquad \text{on } \Gamma, \tag{A.12}$$

Fluid flow and mass balance: Introducing the asymptotic expansions (3.13) in Eqs. (A.1)-(A.2) and (A.7)-(A.8), the first order problem to be solved is given by

$$\nabla_y p^{f(0)} = 0 \qquad \text{in } \Omega^f, \tag{A.13}$$

where the unknown $p^{f(0)}$ is $\mathbf{y}$-periodic. Thus, from Eq. (A.13) we get

$$p^{f(0)} = p^{f(0)}(\mathbf{x}, t). \tag{A.14}$$

Taking into account this result, the second order problem is given by

$$\mu^f \triangle_y \mathbf{v}^{f(0)} - \nabla_y p^{f(1)} - \nabla_x p^{f(0)} = 0 \qquad \text{in } \Omega^f, \tag{A.15}$$

$$\nabla_y \cdot \mathbf{v}^{f(0)} = 0 \qquad \text{in } \Omega^f, \tag{A.16}$$

$$\mathbf{v}^{f(0)} \cdot \mathbf{t} = 0 \qquad \text{on } \Gamma, \tag{A.17}$$

$$\mathbf{v}^{f(0)} \cdot \mathbf{N} = 0 \qquad \text{on } \Gamma, \tag{A.18}$$

This is a boundary-value problem for the $\mathbf{y}$-periodic unknowns $p^{f(1)}$ and $\mathbf{v}^{f(0)}$. From Eq. (A.15)-(A.18), it has been shown [1] that the fluid velocity $\mathbf{v}^{f(0)}$ and the pressure $p^{f(1)}$ can be put in the form

$$\mathbf{v}^{f(0)} = -\mathbf{k}(\mathbf{y}, t) \nabla_x p^{f(0)}, \tag{A.19}$$

$$p^{f(1)} = \mathbf{b}(\mathbf{y}, t) \cdot \nabla_x p^{f(0)} + \overline{p}^{f(1)}(\mathbf{x}, t), \tag{A.20}$$

where $\mathbf{k}(\mathbf{y}, t)$ is the microscopic permeability tensor. The fluid pressure $p^{f(1)}$ is a linear function of the macroscopic gradient $\nabla_x p^{f(0)}$, modulo an arbitrary function $\overline{p}^{f(1)}(\mathbf{x}, t)$. The vector $\mathbf{b}(\mathbf{y}, t)$ is $\mathbf{y}$-periodic and average to zero, $\langle \mathbf{b} \rangle = 0$. The latter condition ensures the uniqueness of $\mathbf{b}$. The microscopic permeability tensor $\mathbf{k}$ and the pore vector field $\mathbf{b}$ are the solutions of the following boundary value problem,

$$\mu^f \triangle_y \mathbf{k} - \nabla_y \mathbf{b} - \boldsymbol{\delta} = 0 \qquad \text{in } \Omega^f, \tag{A.21}$$

$$\nabla_y \cdot \mathbf{k} = 0 \qquad \text{in } \Omega^f, \tag{A.22}$$

$$\mathbf{k} = 0 \qquad \text{on } \Gamma, \tag{A.23}$$

where $\boldsymbol{\delta}$ is the unit tensor.The macroscopic fluid velocity $\langle \mathbf{v}^{f(0)} \rangle$ follows Darcy's law,

$$\langle \mathbf{v}^{f(0)} \rangle = -\mathbf{K} \nabla_x p^{f(0)}, \quad K_{ij} = \frac{1}{\Omega} \int_{\Omega^f} k_{ij}(\mathbf{y}, t) \, d\Omega, \tag{A.24}$$

where $\mathbf{K}$ is the macroscopic permeability tensor. We consider now equations,

$$\nabla_y \cdot \mathbf{v}^{f(1)} + \nabla_x \cdot \mathbf{v}^{f(0)} = 0 \qquad \text{in } \Omega^f, \tag{A.25}$$

$$\mathbf{v}^{f(1)} \cdot \mathbf{t} = 0 \qquad \text{on } \Gamma, \tag{A.26}$$

$$\rho^f (\mathbf{v}^{f(1)} - \mathbf{w}^{(0)}) \cdot \mathbf{N} = -\rho^s \mathbf{w}^{(0)} \cdot \mathbf{N} \qquad \text{on } \Gamma, \tag{A.27}$$

where the unknown $\mathbf{v}^{f(1)}$ is $\mathbf{y}$-periodic. Integrating equation (A.25) over Ω^f and then using the divergence theorem, boundary condition (A.27) and the period-

icity on $\partial\Omega \cap \partial\Omega^f$, we obtain

$$\rho^f \nabla_x \cdot \langle \mathbf{v}^{f(0)} \rangle = -\frac{1}{\Omega} \int_{\Gamma \cup (\partial\Omega \cap \partial\Omega^f)} \rho^f \mathbf{v}^{f(1)} \cdot \mathbf{N} d\Gamma \tag{A.28}$$

$$= -(\rho^f - \rho^s)\frac{1}{\Omega} \int_{\Gamma} \mathbf{w}^{(0)} \cdot \mathbf{N} d\Gamma,$$

with

$$\frac{1}{\Omega} \int_{\Gamma} \mathbf{w}^{(0)} \cdot \mathbf{N} d\Gamma = \frac{d}{dt}\left(\frac{\Omega^f}{\Omega}\right) = \frac{df^f}{dt} = -\frac{df^s}{dt}. \tag{A.29}$$

f^s and f^f are the solid volume fraction and the fluid volume fraction, respectively. Therefore, the macroscopic volume balance takes the form

$$\nabla_x \cdot \langle \mathbf{v}^{f(0)} \rangle + \left(\frac{\rho^s}{\rho^f} - 1\right) \frac{df^s}{dt} = 0. \tag{A.30}$$

Heat transfer: Introducing the asymptotic expansions (3. 13) in Eq. (A.3)-(A.4) and (A.9)-(A. 10), the lower order problem to be solved is given by

$$\nabla_y \cdot \left(\lambda^s \nabla_y T^{s(0)}\right) = 0 \qquad \text{in } \Omega^s, \tag{A.31}$$

$$\nabla_y \cdot \left(\lambda^f \nabla_y T^{f(0)}\right) = 0 \qquad \text{in } \Omega^f, \tag{A.32}$$

$$T^{s(0)} = T^{f(0)} = T^{*(0)} \qquad \text{on } \Gamma, \tag{A.33}$$

$$\left(\lambda^s \nabla_y T^{s(0)} - \lambda^f \nabla_y T^{f(0)}\right) \cdot \mathbf{N} = 0 \qquad \text{on } \Gamma, \tag{A.34}$$

where the unknowns $T^{s(0)}$ and $T^{f(0)}$ are $\mathbf{y}$-periodic. It can be shown that the obvious solution of the above boundary value problem (A.31)-(A.34) is given by

$$T^{s(0)} = T^{f(0)} = T^{*(0)} = T^{(0)}(\mathbf{x}, t). \tag{A.35}$$

It means that the first order solution is independent of the microscopic variable $\mathbf{y}$ and that we have only one temperature field at the first order of approximation. Taking into account the preceding results, we get the following second-order problem:

$$\nabla_y \cdot \left[\lambda^s \left(\nabla_y T^{s(1)} + \nabla_x T^{(0)}\right)\right] = 0 \qquad \text{in } \Omega^s, \tag{A.36}$$

$$\nabla_y \cdot \left[\lambda^f \left(\nabla_y T^{f(1)} + \nabla_x T^{(0)}\right)\right] = 0 \qquad \text{in } \Omega^f, \tag{A.37}$$

$$T^{s(1)} = T^{f(1)} = T^{*(1)} \qquad \text{on } \Gamma, \tag{A.38}$$

$$\left[\lambda^s \left(\nabla_y T^{s(1)} + \nabla_x T^{(0)}\right) - \lambda^f \left(\nabla_y T^{f(1)} + \nabla_x T^{(0)}\right)\right] \cdot \mathbf{N} = 0 \qquad \text{on } \Gamma, \tag{A.39}$$

where the unknowns $T^{s(1)}$ and $T^{f(1)}$ are $\mathbf{y}$-periodic. The solution of the set of equations (A.36)-(A.39) appears as a linear function of the macroscopic thermal gradient of $T^{(0)}$, modulo an arbitrary function $\overline{T}^{(1)}(\mathbf{x}, t)$:

$$T^{(1)} = \boldsymbol{\chi}(\mathbf{y}, t) \cdot \nabla_x T^{(0)} + \overline{T}^{(1)}(\mathbf{x}, t). \tag{A.40}$$

$T^{(1)}$ stands for $T^{s(1)}$ in Ω^s and $T^{f(1)}$ in Ω^f. The vector $\boldsymbol{\chi}(\mathbf{y}, t)$ is $\mathbf{y}$-periodic, average to zero, and it is a solution of the following boundary-value problem:

$$\nabla_y \cdot [\lambda^s (\nabla_y \boldsymbol{\chi} + \boldsymbol{\delta})] = 0 \qquad \text{in } \Omega^s, \tag{A.41}$$

$$\nabla_y \cdot \left[\lambda^f (\nabla_y \boldsymbol{\chi} + \boldsymbol{\delta})\right] = 0 \qquad \text{in } \Omega^f, \tag{A.42}$$

$$\lambda^s (\nabla_y \boldsymbol{\chi} + \boldsymbol{\delta}) \cdot \mathbf{N} = \lambda^f (\nabla_y \boldsymbol{\chi} + \boldsymbol{\delta}) \cdot \mathbf{N} \qquad \text{on } \Gamma, \tag{A.43}$$

The third order problem is given by

$$\rho^s C_p^s \frac{\partial T^{(0)}}{\partial t} - \nabla_y \cdot \left[\lambda^s \left(\nabla_y T^{s(2)} + \nabla_x T^{s(1)}\right)\right] - \nabla_x \cdot \left[\lambda^s \left(\nabla_y T^{s(1)} + \nabla_x T^{(0)}\right)\right] = 0 \quad \text{in} \quad \Omega^s, \tag{A.44}$$

$$\rho^f C_p^f \frac{\partial T^{(0)}}{\partial t} + \rho^f C_p^f \mathbf{v}^{f(0)} \cdot \left(\nabla_y T^{f(1)} + \nabla_x T^{(0)}\right) - \nabla_y \cdot \left[\lambda^f \left(\nabla_y T^{f(2)} + \nabla_x T^{f(1)}\right)\right] - \nabla_x \cdot \left[\lambda^f \left(\nabla_y T^{f(1)} + \nabla_x T^{(0)}\right)\right] = 0 \quad \text{in} \quad \Omega^f, \tag{A.45}$$

$$T^{s(2)} = T^{f(2)} = T^{*(2)} \qquad \text{on} \quad \Gamma, \tag{A.46}$$

$$\left[\lambda^s \left(\nabla_y T^{s(2)} + \nabla_x T^{s(1)}\right) - \lambda^f \left(\nabla_y T^{f(2)} + \nabla_x T^{f(1)}\right)\right] \cdot \mathbf{N} = L^{fs} \rho^s \mathbf{w}^{(0)} \cdot \mathbf{N} \quad \text{on} \quad \Gamma, \tag{A.47}$$

where the $\mathbf{y}$-periodic unknowns are $T^{s(2)}$ and $T^{f(2)}$. The fluid velocity $\mathbf{v}^{f(0)}$ follows the law (A.19). Integrating (A.44) over Ω^s and (A.45) over Ω^f and then using the divergence theorem, the condition of periodicity on $\partial\Omega \cap \partial\Omega^f$ and $\partial\Omega \cap \partial\Omega^s$ and the boundary condition (A.47) leads to first order macroscopic description:

$$(\rho C_p)^{\text{eff}} \frac{\partial T^{(0)}}{\partial t} + \rho^f C_p^f \mathbf{V}_T^{\text{eff}} \cdot \nabla_x T^{(0)} - \nabla_x \cdot \left(\boldsymbol{\lambda}^{\text{eff}} \nabla_x T^{(0)}\right) - L^{fs} \rho^s \frac{df^s}{dt} = 0. \tag{A.48}$$

$(\rho C_p)^{\text{eff}}$ and $\boldsymbol{\lambda}^{\text{eff}}$ are the effective thermal capacity and the effective conductivity tensor of the mixture respectively, and $\mathbf{V}_T^{\text{eff}}$ is the effective fluid velocity. These different effective parameters are defined as follows

$$(\rho C_p)^{\text{eff}} = f^s \rho^s C_p^s + f^f \rho^f C_p^f, \tag{A.49}$$

$$\boldsymbol{\lambda}^{\text{eff}} = \frac{1}{\Omega} \int_{\Omega^f} \lambda^f \left(\nabla_y \boldsymbol{\chi} + \boldsymbol{\delta}\right) d\Omega + \frac{1}{\Omega} \int_{\Omega^s} \lambda^s \left(\nabla_y \boldsymbol{\chi} + \boldsymbol{\delta}\right) d\Omega, \tag{A.50}$$

$$\mathbf{V}_T^{\text{eff}} = \frac{1}{\Omega} \int_{\Omega^f} \mathbf{v}^{f(0)} \left(\nabla_y \boldsymbol{\chi} + \boldsymbol{\delta}\right) d\Omega. \tag{A.51}$$

Species transport:

CASE. $D_l = O(1)$ and $FS_l^s = O(\varepsilon^{-1})$ (Fe-C alloy): Introducing the asymptotic expansions (3.13) in Eqs. (A.5)-(A.6) and (A.11)-(A.12), the first order problem to be solved takes the forms

$$\nabla_y \cdot \left(\rho^s \; D^s \nabla_y \omega^{s(0)}\right) = 0 \qquad \text{in } \Omega^s, \tag{A.52}$$

$$\rho^f \mathbf{v}^{f(0)} \cdot \nabla_y \omega^{f(0)} - \nabla_y \cdot \left(\rho^f \; D^f \nabla_y \omega^{f(0)}\right) = 0 \qquad \text{in } \Omega^f, \tag{A.53}$$

$$\left(\rho^s D^s \nabla_y \omega^{s(0)} - \rho^f D^f \nabla_y \omega^{f(0)}\right) \cdot \mathbf{N} = 0 \qquad \text{on } \Gamma, \tag{A.54}$$

$$\omega^{s*(0)} = k \; \omega^{f*(0)} \qquad \text{on } \Gamma, \tag{A.55}$$

where the unknowns $\omega^{s(0)}$ and $\omega^{f(0)}$ are $\mathbf{y}$-periodic. The fluid $\mathbf{v}^{f(0)}$ velocity follows the law (A.19). From Eqs. (A.52)-(A.55), we get

$$\begin{aligned} \omega^{f(0)} &= \omega^{f*(0)} = \omega^{f(0)}(\mathbf{x}, t), \\ \omega^{s(0)} &= \omega^{s*(0)} = \omega^{s(0)}(\mathbf{x}, t) = k\omega^{f(0)}. \end{aligned} \tag{A.56}$$

At the first order of approximation, the fluid and the solid mass fraction are independent of the microscopic variable $\vec{y}$, i.e. they are constant over the cell. We consider now the following equations that are obtained at a higher order:

$$\rho^s \frac{\partial \omega^{s(0)}}{\partial t} - \nabla_y \cdot \left[\rho^s \; D^s \left(\nabla_y \omega^{s(1)} + \nabla_x \omega^{s(0)}\right)\right] = 0 \qquad \text{in} \quad \Omega^s \tag{A.57}$$

$$\begin{aligned} \rho^f \frac{\partial \omega^{f(0)}}{\partial t} + \rho^f \mathbf{v}^{f(0)} \cdot \left(\nabla_y \omega^{f(1)} + \nabla_x \omega^{f(0)}\right) \\ - \nabla_y \cdot \left[\rho^f \; D^f \left(\nabla_y \omega^{f(1)} + \nabla_x \omega^{f(0)}\right)\right] = 0 \quad \text{in} \quad \Omega^f, \end{aligned} \tag{A.58}$$

$$\left[\rho^s D^s \left(\nabla_y \omega^{s(1)} + \nabla_x \omega^{s(0)}\right) - \rho^f D^f \left(\nabla_y \omega^{f(1)} + \nabla_x \omega^{f(0)}\right)\right] \cdot \mathbf{N} = (\rho^f \omega^{f*(0)} - \rho^s \omega^{s*(0)}) \mathbf{w}^{(0)} \cdot \mathbf{N} \quad \text{on} \quad \Gamma, \tag{A.59}$$

where the unknowns $\omega^{f(1)}$ and $\omega^{s(1)}$ are $\mathbf{y}$-periodic. Integrating (A.57) over Ω^s and (A.58) over Ω^f and then using the divergence theorem, the condition of periodicity on $\partial\Omega \cap \partial\Omega^f$ and $\partial\Omega \cap \partial\Omega^s$ leads to

$$|\Omega^s| \rho^s \frac{\partial \omega^{s(0)}}{\partial t} - \int_\Gamma \rho^s \; D^s \left(\nabla_y \omega^{s(1)} + \nabla_x \omega^{s(0)}\right) \cdot \mathbf{N} d\Gamma = 0, \tag{A.60}$$

$$|\Omega^f| \rho^f \frac{\partial \omega^{f(0)}}{\partial t} + \rho^f \int_{\Omega^f} \mathbf{v}^{f(0)} \cdot \left(\nabla_y \omega^{f(1)} + \nabla_x \omega^{f(0)}\right) d\Omega - \int_\Gamma \rho^f \; D^f \left(\nabla_y \omega^{f(1)} + \nabla_x \omega^{f(0)}\right) \cdot \mathbf{N} d\Gamma = 0. \tag{A.61}$$

By considering the fluid incompressibility (A.16) and the boundary condition (A.18), and by using the divergence theorem and the periodicity on $\partial\Omega \cap \partial\Omega^f$, we get

$$\int_{\Omega^f} \mathbf{v}^{f(0)} \cdot \nabla_y \omega^{f(1)} d\Omega = 0. \tag{A.62}$$

Therefore, from Eqs. (A.60)-(A.61) and the boundary condition (A.59), we obtain the following first order macroscopic description

$$\rho^s \frac{\partial \left(f^s k \; \omega^{f(0)}\right)}{\partial t} + \rho^f \frac{\partial \left((1 - f^s) \omega^{f(0)}\right)}{\partial t} + \rho^f \langle \mathbf{v}^{f(0)} \rangle \cdot \nabla_x \omega^{f(0)} = 0, \tag{A.63}$$

where $\langle \mathbf{v}^{f(0)} \rangle = -\mathbf{K} \; \nabla_x p^{f(0)}$ and $\omega^{s(0)}(\mathbf{x}, t) = k \; \omega^{f(0)}(\mathbf{x}, t)$.

CASE. $D_l = O(\varepsilon)$ and $FS_l^s = O(1)$ (Sn-Pb alloy): The first order problem to be solved takes now the forms:

$$\rho^s \frac{\partial \omega^{s(0)}}{\partial t} - \nabla_y \cdot \left(\rho^s \; D^s \nabla_y \omega^{s(0)}\right) = 0 \qquad \text{in } \Omega^s, \tag{A.64}$$

$$\rho^f \mathbf{v}^{f(0)} \nabla_y \omega^{f(0)} - \nabla_y \cdot \left(\rho^f \; D^f \nabla_y \omega^{f(0)}\right) = 0 \qquad \text{in } \Omega^f, \tag{A.65}$$

$$\rho^f D^f \nabla_y \omega^{f(0)} \cdot \mathbf{N} = 0 \qquad \text{on } \Gamma, \tag{A.66}$$

$$\omega^{s*(0)} = k \; \omega^{f*(0)} \qquad \text{on } \Gamma, \tag{A.67}$$

where the unknowns $\omega^{s(0)}$ and $\omega^{f(0)}$ are $\mathbf{y}$-periodic. The fluid $\mathbf{v}^{f(0)}$ velocity follows the law (A.19). Once again, from Eqs. (A.65)-(A.66), we get: $\omega^{f(0)} = \omega^{f*(0)} = \omega^{f(0)}(\mathbf{x}, t)$. At the first order of approximation, the fluid mass fraction is independent of the microscopic variable $\mathbf{y}$. In contrast with $\omega^{f(0)}$, the solid mass fraction is $\mathbf{y}$-dependent. Consider a solid mass fraction in the form $\omega^{s(0)}(\mathbf{x}, \mathbf{y}, t) = \overline{\omega}^{s(0)}(\mathbf{x}, \mathbf{y})\, e^{i\omega t}$ and the Fourier transform of Eqs. (A.64) and (A.67). The Fourier transform $\overline{\omega}^{s(0)}$ of $\omega^{s(0)}$ appears as a linear function of the fluid mass fraction,

$$\overline{\omega}^{s(0)} = \phi(\omega, \mathbf{y})\ \omega^{f(0)}(\mathbf{x}, t). \tag{A.68}$$

The complex function $\phi(\omega, \mathbf{y})$ is the $\mathbf{y}$-periodic solution of the following boundary value problem:

$$-\rho^s i\ \omega\ \phi - \nabla_y \cdot (\rho^s\ D^s \nabla_y \phi) = 0 \qquad \text{in } \Omega^s, \tag{A.69}$$

$$\phi = k \qquad \text{on } \Gamma. \tag{A.70}$$

We consider now the following equations that are obtained at a higher order:

$$\rho^f \frac{\partial \omega^{f(0)}}{\partial t} + \rho^f \mathbf{v}^{f(0)} \cdot \left(\nabla_y \omega^{f(1)} + \nabla_x \omega^{f(0)}\right) - \nabla_y \cdot \left[\rho^f\ D^f \left(\nabla_y \omega^{f(1)} + \nabla_x \omega^{f(0)}\right)\right] = 0 \quad \text{in } \Omega^f, \tag{A.71}$$

$$\left[\rho^s D^s \nabla_y \omega^{s(0)} - \rho^f D^f \left(\nabla_y \omega^{f(1)} + \nabla_x \omega^{f(0)}\right)\right] \cdot \mathbf{N} = \rho^f \omega^{f*(0)} - \rho^s \omega^{s*(0)}) \mathbf{w}^{(0)} \cdot \mathbf{N} \quad \text{on } \Gamma, \tag{A.72}$$

where the unknown $\omega^{f(1)}$ is $\mathbf{y}$-periodic. The relation (A.62) remains valid. Therefore, integrating (A.64) over Ω^s and (A.71) over Ω^f and then using the divergence theorem, the condition of periodicity on $\partial\Omega \cap \partial\Omega^f$ and on $\partial\Omega \cap \partial\Omega^s$ and the boundary condition (A.72) leads to the following first order macroscopic description:

$$\rho^s \left(\left\langle \frac{\partial \omega^{s(0)}}{\partial t} \right\rangle + \frac{\mathrm{d} f^s}{\mathrm{d} t} \omega^{s*(0)}\right) + \rho^f\ \frac{\partial \left((1 - f^s)\omega^{f(0)}\right)}{\partial t} + \rho^f \langle \mathbf{v}^{f(0)} \rangle \cdot \nabla_x \omega^{f(0)} = 0, \tag{A.73}$$

where $\langle \mathbf{v}^{f(0)} \rangle = -\mathbf{K}\ \nabla_x p^{f(0)}$ and $\omega^{s*(0)}(\mathbf{x}, t) = k\ \omega^{f(0)}(\mathbf{x}, t)$. We have

$$F\left(\left\langle \frac{\partial \omega^{s(0)}}{\partial t} \right\rangle\right) = \frac{1}{\Omega} \int_{\Omega^s} i\ \omega \phi(\omega, \mathbf{y})\ d\Omega\ .\omega^{f(0)} = \Phi(\omega).\omega^{f(0)} \tag{A.74}$$

where $F\left(\left\langle \frac{\partial \omega^{s(0)}}{\partial t} \right\rangle\right)$ is the Fourier transform of $\left\langle \frac{\partial \omega^{s(0)}}{\partial t} \right\rangle$. $\Phi(\omega)$ is a complex effective coefficient. From Eq. (A.74), it follows

$$\left\langle \frac{\partial \omega^{s(0)}}{\partial t} \right\rangle = F^{-1}(\Phi(\omega)) * \omega^{f(0)} \tag{A.75}$$

where $F^{-1}(\Phi(\omega))$ in the inverse Fourier transform of $\Phi(\omega)$ and $*$ is the convolution product.

Appendix B. Model B

Species transport: We now consider the order of magnitude of dimensionless numbers given in Table 2 for model B. The dimensionless description concerning the species transport takes the forms

$$(FS_l^s)^{-1}\ \rho^s \frac{\partial \omega^s}{\partial t} - \nabla \cdot (\rho^s D^s \nabla \omega^s) = 0 \qquad \text{in } \Omega^s, \tag{B.1}$$

$$\varepsilon^2\ \rho^f \frac{\partial \omega^f}{\partial t} + \varepsilon \rho^f \vec{v}^f \cdot \nabla \omega^f - \nabla \cdot (\rho^f D^f \nabla \omega^f) = 0 \qquad \text{in } \Omega^f, \tag{B.2}$$

$$\left((D_l)\rho^s D^s \nabla \omega^s - \rho^f D^f \nabla \omega^f\right) \cdot \mathbf{N} = \varepsilon^2 (\rho^f \omega^{f*} - \rho^s \omega^{s*}) \mathbf{w} \cdot \mathbf{N} \qquad \text{on } \Gamma, \tag{B.3}$$

$$\omega^{s*} = k\ \omega^{f*} \qquad \text{on } \Gamma. \tag{B.4}$$

Consider the case $D_l = O(1)$ and $FS_l^s = O(\varepsilon^{-2})$ (Fe-C alloy). Introduction of the asymptotic expansions (3.13) in Eqs. (B.1)-(B.4), yields at the lower order problem:

$$\nabla_y \cdot \left(\rho^s D^s \nabla_y \omega^{s(0)}\right) = 0 \qquad \text{in } \Omega^s, \tag{B.5}$$

$$\nabla_y \cdot \left(\rho^f D^f \nabla_y \omega^{f(0)}\right) = 0 \qquad \text{in } \Omega^f, \tag{B.6}$$

$$\left(\rho^s D^s \nabla_y \omega^{s(0)} - \rho^f D^f \nabla_y \omega^{f(0)}\right) \cdot \mathbf{N} = 0 \qquad \text{on } \Gamma, \tag{B.7}$$

$$\omega^{s*(0)} = k\ \omega^{f*(0)} \qquad \text{on } \Gamma. \tag{B.8}$$

where the unknowns $\omega^{s(0)}$ and $\omega^{f(0)}$ are $\mathbf{y}$-periodic. From Eqs. (B.5)-(B.8), we get

$$\begin{aligned} \omega^{f(0)} &= \omega^{f*(0)} = \omega^{f(0)}(\mathbf{x}, t), \\ \omega^{s(0)} &= \omega^{s*(0)} = \omega^{s(0)}(\mathbf{x}, t) = k\ \omega^{f(0)}(\mathbf{x}, t). \end{aligned} \tag{B.9}$$

At the first order, the solid and the fluid mass fraction are constant over the periodic cell (lever-rule type model). The second order problem to be solved

takes the form:

$$\nabla_y \cdot \left[\rho^s \; D^s \left(\nabla_y \omega^{s(1)} + \nabla_x \omega^{s(0)}\right)\right] = 0 \quad \text{in } \Omega^s \tag{B.10}$$

$$\nabla_y \cdot \left[\rho^f \; D^f \left(\nabla_y \omega^{f(1)} + \nabla_x \omega^{f(0)}\right)\right] = 0 \quad \text{in } \Omega^f, \tag{B.11}$$

$$\left[\rho^s D^s \left(\nabla_y \omega^{s(1)} + \nabla_x \omega^{s(0)}\right) - \rho^f D^f \left(\nabla_y \omega^{f(1)} + \nabla_x \omega^{f(0)}\right)\right] \cdot \mathbf{N} = 0 \quad \text{on } \Gamma, \tag{B.12}$$

$$\omega^{s*(1)} = k \; \omega^{f*(1)} \quad \text{on } \Gamma, \tag{B.13}$$

where the unknowns $\omega^{s(1)}$ and $\omega^{f(1)}$ are $\mathbf{y}$-periodic. The solutions of the set of Eqs. (B.10)-(B.13) appear as a linear function of the macroscopic solutal gradient of $\omega^{f(0)}$, modulo an arbitrary function,

$$\omega^{f(1)} = \boldsymbol{\beta}^f(\mathbf{y}, t) \cdot \nabla_x \omega^{f(0)} + \overline{\omega}^{f(1)}(\mathbf{x}, t), \tag{B.14}$$

$$\omega^{s(1)} = k \; \boldsymbol{\beta}^s(\mathbf{y}, t) \cdot \nabla_x \omega^{f(0)} + \overline{\omega}^{s(1)}(\mathbf{x}, t). \tag{B.15}$$

$\boldsymbol{\beta}^f(\mathbf{y}, t)$ and $\boldsymbol{\beta}^s(\mathbf{y}, t)$ are $\mathbf{y}$-periodic, average to zero, and are solutions of the following boundary-value problem:

$$\nabla_y \cdot [\rho^s D^s k \; (\nabla_y \boldsymbol{\beta}^s + \delta)] = 0 \quad \text{in } \Omega^s, \tag{B.16}$$

$$\nabla_y \cdot \left[\rho^f D^f \left(\nabla_y \boldsymbol{\beta}^f + \delta\right)\right] = 0 \quad \text{in } \Omega^f, \tag{B.17}$$

$$\rho^s D^s k \; (\nabla_y \boldsymbol{\beta}^s + \delta) \cdot \mathbf{N} = \rho^f D^f \left(\nabla_y \boldsymbol{\beta}^f + \delta\right) \cdot \mathbf{N} \quad \text{on } \Gamma. \tag{B.18}$$

$$\boldsymbol{\beta}^s = \boldsymbol{\beta}^f \quad \text{on } \Gamma, \tag{B.19}$$

The third order order problem to be solved is given by

$$\rho^s \frac{\partial \omega^{s(0)}}{\partial t} - \nabla_y \cdot \left[\rho^s D^s \left(\nabla_y \omega^{s(2)} + \nabla_x \omega^{s(1)}\right)\right] - \nabla_x \cdot \left[\rho^s D^s \left(\nabla_y \omega^{s(1)} + \nabla_x \omega^{s(0)}\right)\right] = 0 \quad \text{in } \Omega^s, \tag{B.20}$$

$$\text{(B.21)}\quad \rho^f \frac{\partial \omega^{f(0)}}{\partial t} + \rho^f \mathbf{v}^{f(0)} \cdot \left(\nabla_y \omega^{f(1)} + \nabla_x \omega^{f(0)}\right) - \nabla_y \cdot \left[\rho^f D^f \left(\nabla_y \omega^{f(2)} + \nabla_x \omega^{f(1)}\right)\right] - \nabla_x \cdot \left[\rho^f D^f \left(\nabla_y \omega^{f(1)} + \nabla_x \omega^{f(0)}\right)\right] = 0 \quad \text{in } \Omega^f,$$

$$\text{(B.22)}\quad \left[\rho^s D^s \left(\nabla_y \omega^{s(2)} + \nabla_x \omega^{s(1)}\right) - \rho^f D^f \left(\nabla_y \omega^{f(2)} + \nabla_x \omega^{f(1)}\right)\right] \cdot \mathbf{N} = (\rho^f \omega^{f*(0)} - \rho^s \omega^{s*(0)}) \mathbf{w}^{(0)} \cdot \mathbf{N} \quad \text{on } \Gamma.$$

Integrating (B.20) over Ω^s and (B.21) over Ω^f, using the divergence theorem, the condition of periodicity on $\partial\Omega \cap \partial\Omega^f$ and $\partial\Omega \cap \partial\Omega^s$, and then taking into account the boundary condition (B.22), leads to the following first order macroscopic description

$$\text{(B.23)}\quad \rho^s \frac{\partial \left(f^s k\, \omega^{f(0)}\right)}{\partial t} + \rho^f \frac{\partial \left((1 - f^s)\omega^{f(0)}\right)}{\partial t} + \rho^f \mathbf{V}_S^{\text{eff}} \cdot \nabla_x \omega^{f(0)} - \nabla_x \cdot \left((\rho \mathbf{D}^\star) \nabla_x \omega^{f(0)}\right) = 0.$$

with $\omega^{s(0)}(\mathbf{x}, t) = k\, \omega^{f(0)}(\mathbf{x}, t)$. The effective diffusion tensor $(\rho \mathbf{D}^\star)$ of the mixture and the effective fluid velocity $\mathbf{V}_S^{\text{eff}}$ are defined as follows:

$$\text{(B.24)}\quad \mathbf{V}_S^{\text{eff}} = \frac{1}{\Omega} \int_{\Omega^f} \mathbf{v}^{f(0)} \left(\nabla_y \boldsymbol{\beta}^f + \boldsymbol{\delta}\right) d\Omega,$$

$$\text{(B.25)}\quad (\rho \mathbf{D}^\star) = \frac{1}{\Omega} \int_{\Omega^f} \rho^f D^f \left(\nabla_y \boldsymbol{\beta}^f + \boldsymbol{\delta}\right) d\Omega + \frac{1}{\Omega} \int_{\Omega^s} \rho^s D^s \left(\nabla_y \boldsymbol{\beta}^s + k\, \boldsymbol{\delta}\right) d\Omega.$$

Appendix C. Model C

Species transport: We now consider the order of magnitude of dimensionless numbers given in Table 2, model C. The set of dimensionless equations takes the form:

$$\text{(C.1)}\quad (FS_l^s)^{-1}\, \rho^s \frac{\partial \omega^s}{\partial t} - \nabla \cdot (\rho^s D^s \nabla \omega^s) = 0 \quad \text{in } \Omega^s,$$

$$\text{(C.2)}\quad \varepsilon^2\, \rho^f \frac{\partial \omega^f}{\partial t} + \rho^f \mathbf{v}^f \cdot \nabla \omega^f - \nabla \cdot (\rho^f D^f \nabla \omega^f) = 0 \quad \text{in } \Omega^f,$$

$$\text{(C.3)}\quad \left((D_l)\, \rho^s D^s \nabla \omega^s - \rho^f D^f \nabla \omega^f\right) \cdot \mathbf{N} = \varepsilon^2 (\rho^f \omega^{f*} - \rho^s \omega^{s*}) \mathbf{w} \cdot \mathbf{N} \quad \text{on } \Gamma,$$

$$\text{(C.4)}\quad \omega^{s*} = k\, \omega^{f*} \quad \text{on } \Gamma.$$

Consider the case $D_l = O(1)$ and $FS_l^s = O(\varepsilon^{-2})$ (Fe-C alloy). Introducing the asymptotic expansions (3.13) in Eqs. (C.1)-(C.4), the first order problem to be solved takes the form

$$\nabla_y \cdot \left(\rho^s D^s \nabla_y \omega^{s(0)}\right) = 0 \qquad \text{in } \Omega^s, \tag{C.5}$$

$$\rho^f \mathbf{v}^{f(0)} \cdot \nabla_y \omega^{f(0)} - \nabla_y \cdot \left(\rho^f D^f \nabla_y \omega^{f(0)}\right) = 0 \qquad \text{in } \Omega^f, \tag{C.6}$$

$$\left(\rho^s D^s \nabla_y \omega^{s(0)} - \rho^f D^f \nabla_y \omega^{f(0)}\right) \cdot \mathbf{N} = 0 \qquad \text{on } \Gamma, \tag{C.7}$$

$$\omega^{s*(0)} = k\, \omega^{f*(0)} \qquad \text{on } \Gamma, \tag{C.8}$$

where the unknowns $\omega^{s(0)}$ and $\omega^{f(0)}$ are $\mathbf{y}$-periodic. The fluid $\mathbf{v}^{f(0)}$ velocity is given by Eq. (A.19). From Eqs. (C.5)-(C.8), we get

$$\omega^{f(0)} = \omega^{f*(0)} = \omega^{f(0)}(\mathbf{x}, t), \qquad \omega^{s(0)} = \omega^{s*(0)} = \omega^{s(0)}(\mathbf{x}, t). \tag{C.9}$$

At the lower order, the fluid and the solid mass fractions are constant over the cell. We consider now the next order,

$$\nabla_y \cdot \left[\rho^s D^s \left(\nabla_y \omega^{s(1)} + \nabla_x \omega^{s(0)}\right)\right] = 0 \quad \text{in } \Omega^s \tag{C.10}$$

$$\rho^f \mathbf{v}^{f(0)} \cdot \left(\nabla_y \omega^{f(1)} + \nabla_x \omega^{f(0)}\right) - \nabla_y \cdot \left[\rho^f D^f \left(\nabla_y \omega^{f(1)} + \nabla_x \omega^{f(0)}\right)\right] = 0 \quad \text{in } \Omega^f, \tag{C.11}$$

$$\left[\rho^s D^s \left(\nabla_y \omega^{s(1)} + \nabla_x \omega^{s(0)}\right) - \rho^f D^f \left(\nabla_y \omega^{f(1)} + \nabla_x \omega^{f(0)}\right)\right] \cdot \mathbf{N} = 0 \quad \text{on } \Gamma, \tag{C.12}$$

$$\omega^{s*(1)} = k\, \omega^{f*(1)} \quad \text{on } \Gamma, \tag{C.13}$$

where the unknowns $\omega^{f(1)}$ and $\omega^{s(1)}$ are $\mathbf{y}$-periodic. Integrating (C.10) over Ω^s and (C.11) over Ω^f, the condition of periodicity, the boundary condition (C.12) and the fluid incompressibility (A.16) we obtain the following first order macroscopic description,

$$\rho^f \langle \mathbf{v}^{f(0)} \rangle \cdot \nabla_x \omega^{f(0)} = 0. \tag{C.14}$$

From Eqs.(C.10)-(C.11), we get

$$\omega^{f(1)} = \boldsymbol{\varphi}^f(\mathbf{y}, \nabla_x p^{f(0)}, t) \cdot \nabla_x \omega^{f(0)} + \overline{\omega}^{f(1)}(\mathbf{x}, t), \tag{C.15}$$

$$\omega^{s(1)} = k\ \boldsymbol{\varphi}^s(\mathbf{y}, \nabla_x p^{f(0)}, t) \cdot \nabla_x \omega^{f(0)} + \overline{\omega}^{s(1)}(\mathbf{x}, t). \tag{C.16}$$

$\boldsymbol{\varphi}^f$ and $\boldsymbol{\varphi}^s$ depend on the macroscopic pressure gradient $\nabla_x p^{f(0)}$. They are $\mathbf{y}$-periodic, average zero and are solutions of the following boundary-value problem:

$$\nabla_y \cdot [\rho^s D^s k\ (\nabla_y \boldsymbol{\varphi}^s + \delta)] = 0 \qquad \text{in } \Omega^s, \tag{C.17}$$

$$\mathbf{v}^{f(0)} \cdot \left(\nabla_y \boldsymbol{\varphi}^f + \delta\right) - \nabla_y \cdot \left[\rho^f D^f \left(\nabla_y \boldsymbol{\varphi}^f + \delta\right)\right] = 0 \qquad \text{in } \Omega^f, \tag{C.18}$$

$$\left[\rho^s D^s k\,(\nabla_y \boldsymbol{\varphi}^s + \delta) - \rho^f D^f \left(\nabla_y \boldsymbol{\varphi}^f + \delta\right)\right] \cdot \mathbf{N} = 0 \qquad \text{on } \Gamma, \tag{C.19}$$

$$\boldsymbol{\varphi}^s = \boldsymbol{\varphi}^f \qquad \text{on } \Gamma. \tag{C.20}$$

The next problem to be solved takes the form

$$\rho^s \frac{\partial \omega^{s(0)}}{\partial t} - \nabla_y \cdot \left[\rho^s D^s \left(\nabla_y \omega^{s(2)} + \nabla_x \omega^{s(1)}\right)\right] - \nabla_x \cdot \left[\rho^s D^s \left(\nabla_y \omega^{s(1)} + \nabla_x \omega^{s(0)}\right)\right] = 0 \quad \text{in } \Omega^s, \tag{C.21}$$

$$\rho^f \frac{\partial \omega^{f(0)}}{\partial t} + \rho^f \mathbf{v}^{f(0)} \cdot \left(\nabla_y \omega^{f(2)} + \nabla_x \omega^{f(1)}\right) + \rho^f \mathbf{v}^{f(1)} \cdot \left(\nabla_y \omega^{f(1)} + \nabla_x \omega^{f(0)}\right) - \nabla_y \cdot \left[\rho^f D^f \left(\nabla_y \omega^{f(2)} + \nabla_x \omega^{f(1)}\right)\right] - \nabla_x \cdot \left[\rho^f D^f \left(\nabla_y \omega^{f(1)} + \nabla_x \omega^{f(0)}\right)\right] = 0 \quad \text{in } \Omega^f, \tag{C.22}$$

$$\left[\rho^s D^s \left(\nabla_y \omega^{s(1)} + \nabla_x \omega^{s(0)}\right) - \rho^f D^f \left(\nabla_y \omega^{f(2)} + \nabla_x \omega^{f(1)}\right)\right] \cdot \mathbf{N} = (\rho^f \omega^{f*(0)} - \rho^s \omega^{s*(0)}) \mathbf{w}^{(0)} \cdot \mathbf{N} \quad \text{on } \Gamma. \tag{C.23}$$

Integrating (C.21) over Ω^s and (C.22) over Ω^f, then using the divergence theorem, the condition of periodicity and then taking into account the boundary condition (C.23), we obtain the first order correction to the macroscopic description (C.14),

$$\rho^s \frac{\partial \left(f^s k\ \omega^{f(0)}\right)}{\partial t} + \rho^f \frac{\partial \left((1 - f^s)\omega^{f(0)}\right)}{\partial t} + \rho^f \langle \mathbf{v}^{f(0)} \rangle \cdot \nabla_x \overline{\omega}^{f(1)} + \rho^f \langle \mathbf{v}^{f(1)} \rangle \cdot \nabla_x \omega^{f(0)} - \nabla_x \cdot \left((\rho \mathbf{D}^{**}) \nabla_x \omega^{f(0)}\right) = 0. \tag{C.24}$$

$(\rho\mathbf{D}^{\star\star})$ is the effective dispersion tensor of the mixture,

$$(\text{C.25}) \quad (\rho\mathbf{D}^{\star\star}) = \frac{1}{\Omega}\int_{\Omega^f}\left(\rho^f D^f\left(\nabla_y\boldsymbol{\varphi}^f + \boldsymbol{\delta}\right) + \rho^f k\nabla_x p^{f(0)}\cdot\boldsymbol{\varphi}^f\right)\,d\Omega$$

$$+\frac{1}{\Omega}\int_{\Omega^s}\rho^s D^s k\;\left(\nabla_y\boldsymbol{\varphi}^s + \boldsymbol{\delta}\right)d\Omega.$$

By adding, member to member, Eqs. (C.14) and (C.24) multiplied by ε, we get the second order macroscopic equation governing the average fluid mass fraction $\langle\omega^f\rangle = \langle\omega^{f(0)}\rangle + \varepsilon\langle\omega^{f(1)}\rangle$,

$$(\text{C.26}) \quad \varepsilon\,\rho^s\frac{\partial\left(f^s k\,\langle\omega^f\rangle\right)}{\partial t} + \varepsilon\,\rho^f\frac{\partial\left((1-f^s)\langle\omega^f\rangle\right)}{\partial t} + \rho^f\langle\mathbf{v}^f\rangle\cdot\nabla_x\langle\omega^f\rangle$$

$$-\varepsilon\,\nabla_x\cdot\left((\rho\mathbf{D}^{\star\star})\nabla_x\langle\omega^f\rangle\right) = 0$$

with $\langle\omega^s\rangle = k\,\langle\omega^f\rangle$.

References

1. J.-L. AURIAULT, *Heterogeneous medium is an equivalent description possible?* Int. J. Engng. Sci., **29**, 785–795, 1991.
2. J.-L. AURIAULT and P.M. ADLER, *Taylor dispersion in porous media. Analysis by multiple sacle expansions,* Advances in Water Resources., **18**, 217–226, 1995.
3. J.-L. AURIAULT, *Non saturated deformable porous media: Quasistatics,* Transport in Porous Media, **2**, 45–64, 1987.
4. C. BECKERMANN and R. VISKANTA, *Natural convection solid/liquid phase change in porous media,* Int. J. Heat Mass Transfer, **31**, 35–46, 1988.
5. W. D. BENNON and F. P. INCROPERA, *A continuum model fo momentum, heat and species transport in binary solid-liquid phase change systems. - I. Model formulation,* Int. J. Heat. Mass. Transfer, **30**, 2161–2170, 1987.
6. A. BENSOUSSAN, J.L. LIONS, and G. PAPANICOLAOU, *Asymptotic analysis for periodic structures,* North-Holland, Amsterdam 1978.
7. G. W. BERGANTZ, *Conjugate solidification and melting in multicomponent open and closed system,* Int. J. Heat Mass Transfer, **35**, 533–543, 1992.
8. A. BOUDDOUR, J.-L. AURIAULT, M. MHAMDI-ALAOUI, and J.-F. BLOCH, *Heat and mass transfer in wet porous media in presence of evaporation-condensation,* Int. J. Heat Mass Transfer, **41**, 2263–2277, 1998.
9. M. C. FLEMINGS, *Solidification Processing,* McGraw Hill, New-York 1974.
10. S. GANESAN and D. R. POIRIER, *Conservation of mass and momentum for the flow of interdendritic liquid during solidification,* Metall. Trans. B, **21B**, 173–180, 1990.

11. C. GEINDREAU and J.-L. AURIAULT, *Investigation of the mechanical behaviour of alloys in the semi-solid state by homogenization,* Mech. Mater., **31**, 535–551, 1999.

12. R. HILL, D. LOPER, and P. ROBERTS, *A thermodynamically consistent model of a mushy zone,* Q. J. Mech. Appl. Math., **36**, 505–539, 1983.

13. M. D. JACKSON and M. J. CHEADLE, *A continuum model for the transport of heat, mass and momentum in deformable multicomponent mush, undergoing solid-liquid phase change,* Int. J. Heat Mass Transfer, **41**, 1035–1048, 1998.

14. I. KECECIOGLU and B. RUBINSKY, *A continuum model for propagation of discrete phase-change fronts in porous media in the presence of coupled heat flow, fluid flow and species transport processes,* Int. J. Heat Mass Transfer, **32**, 1111–1130, 1989.

15. M. J. M. KRANE and F. P. INCROPERA, *Analysis of the effect of shrinkage on macrosegregation in alloy solidification,* Metall. and Mater. Trans. A, **26A**, 2329–2388, 1995.

16. S. LE CORRE, D. CAILLERIE, D. FAVIER and L. ORGEAS, *Overall behaviour of a truss of fibres linked by viscous joints,* [in:] FRC 2000 - Composites for the Millenium, A. G. GIBSON [Ed.] Woodhead Publishing Limited vol:1, 303-310, 2000.

17. C. C. MEI and J. L. AURIAULT, *The effect of inertia on flow through porous medium,* J. Fluid. Mech., **222**, 647–663, 1991.

18. I. NASTAC and D. M. STEFANESCU, *Macrotransport solidification kinetics modeling of equiaxed dendritic growth : Part i. Model development and discussion,* Metall. and Mater. Trans. A, **27A**, 4061–4074, 1996.

19. J. NI and C. BECKERMANN, *A volume averaged two-phase model for transport phenomena during solidification,* Metall. Trans. B, **22B**, 349–361, 1991.

20. P. J. PRESCOTT and F. P. INCROPERA, *Convection heat and mass transfer in alloy solidification,* Advances in Heat Transfer, **28**, 231–337, 1996.

21. P. J. PRESCOTT, F. P. INCROPERA, and W. D. BENNON, *Modeling of dendritic solidification systems : Reassessment of the continuum momentum equation,* Int. J. Heat Mass Transfer, **34**, 2351–2359, 1991.

22. M. RAPPAZ and V. VOLLER, *Modeling of micro-macrosegregation in solidification processes,* Metall. Trans. A, **21A**, 749–753, 1990.

23. S. RIDDER, S. KOU, and R. MEHRABIAN, *Effect of fluid flow on macrosegregation in axisymmetric lingots,* Met. Trans. B, **12B**, 435–447, 1981.

24. E. SANCHEZ-PALENCIA. *Non-homogeneous media and vibration theory,* [in:] Lectures Notes in Physics, Vol. 127, Springer-Verlag, Berlin 1980

25. M. C. SCHNEIDER and C. BECKERMANN, *Formation of macrosegregation by multicomponent thermosolutal convection during the solidification of steel,* Metal. Mater. Trans. A, **26A**, 2373–2388, 1995.

26. M. C. SCHNEIDER and C. BECKERMANN, *A numerical study of the combined effects of microsegregation, mushy zone permeability and flow, caused by volume contraction and thermosolutal convection, on macrosegregation and eutectic formation in binary alloy solidification,* Int. J. Heat Mass Transfer, **38**, 3455–3473, 1995.

27. E. SKJETNE and J.-L. AURIAULT, *High-velocity laminar and turbulent flow in porous media,* Transport in Porous Media, **36**, 131–147, 1999.

28. J. SZEKELY and A. JASSAL, *An experimental and analytical study of the solidification of a binary dendritic system,* Metal. Trans. B, **9B**, 389–398, 1978.

29. R. VISKANTA and C. BECKERMANN, *Mathematical modeling of solidification,* Proc. symp. on interdisciplinary issues in materials processing and manufacturing, Boston 1987.

30. V. R. VOLLER, A. D. BRENT, and C. PRAKASH, *The modelling of heat, mass and solute transport in solidification systems,* Int. J. Heat Mass Transfer, **32**, 1719–1731, 1989.

31. M. WORSTER, *Natural convection in a mushy layer,* J. Fluid. Mech., **224**, 335–359, 1991.

32. R. WRIGHT, *Core melt progression : Status of current understanding and principal uncertainties,* U.K. J. ROGERS [Ed.] Heat and Mass Transfer in Severe Nuclear Reactor Accidents, Begell House, New York, Wallingford 1996.

Received March 20, 2001; revised version June 6, 2001.